

Towards clarifying the possibility of observation of the LHCb
hidden-charm pentaquarks
 $P_c^+(4312)$, $P_c^+(4337)$, $P_c^+(4440)$ and $P_c^+(4457)$
in near-threshold charmonium photoproduction off protons
and nuclei

E. Ya. Paryev

*Institute for Nuclear Research, Russian Academy of Sciences,
Moscow 117312, Russia*

Abstract

We study the near-threshold J/ψ meson photoproduction from protons and nuclei by considering incoherent direct non-resonant ($\gamma p \rightarrow J/\psi p$, $\gamma n \rightarrow J/\psi n$) and two-step resonant ($\gamma p \rightarrow P_{ci}^+ \rightarrow J/\psi p$, $\gamma n \rightarrow P_{ci}^0 \rightarrow J/\psi n$, $i = 1, 2, 3, 4$; $P_{c1}^{+,0} = P_c^{+,0}(4312)$, $P_{c2}^{+,0} = P_c^{+,0}(4337)$, $P_{c3}^{+,0} = P_c^{+,0}(4440)$, $P_{c4}^{+,0} = P_c^{+,0}(4457)$) charmonium production processes. We calculate the absolute excitation functions, energy and momentum distributions for the non-resonant, resonant and for the combined (non-resonant plus resonant) production of J/ψ mesons on protons as well as, using the nuclear spectral function approach, on carbon and tungsten target nuclei at near-threshold incident photon energies by assuming the spin-parity assignments of the hidden-charm resonances $P_c^{+,0}(4312)$, $P_c^{+,0}(4337)$, $P_c^{+,0}(4440)$ and $P_c^{+,0}(4457)$ as $J^P = (1/2)^-$, $J^P = (1/2)^-$, $J^P = (1/2)^-$ and $J^P = (3/2)^-$ within three different realistic scenarios for the branching ratios of their decays to the $J/\psi p$ and $J/\psi n$ modes (0.25, 0.5 and 1%). We show that will be very hard to measure the P_{ci}^+ pentaquark states through the scan of the J/ψ total photoproduction cross section on a proton target in the near-threshold energy region around the resonant photon energies of 9.44, 9.554, 10.04 and 10.12 GeV if these branching ratios $\sim 1\%$ and less. We also demonstrate that at these photon beam energies the J/ψ energy and momentum combined distributions considered reveal distinct sensitivity to the above scenarios, respectively, at "low" J/ψ total energies and momenta, which implies that they may be an important tool to provide further evidence for the existence of the pentaquark P_{ci}^+ and P_{ci}^0 resonances and to get valuable information on their decay rates to the $J/\psi p$ and $J/\psi n$ final states. The measurements of these distributions could be performed in the future at the 12 GeV CEBAF facility.

1. Introduction

The study of the exotic hadronic states – the hidden-charm pentaquark resonances – has received considerable interest in recent years and is one of the most exciting topics of the nuclear and hadronic physics nowadays after the discovery by the LHCb Collaboration pentaquark states $P_c^+(4380)$ and $P_c^+(4450)$ in the $J/\psi p$ invariant mass spectrum of the $\Lambda_b^0 \rightarrow K^-(J/\psi p)$ decays [1] and, especially, after the observation by the Collaboration of three new narrow resonances $P_c^+(4312)$, $P_c^+(4440)$ and $P_c^+(4457)$ in these decays [2], based on additional collected data and on an improved selection strategy, instead of initially claimed $P_c^+(4380)$ and $P_c^+(4450)$ states. Very recently, the LHCb Collaboration discovered a new narrow hidden-charm pentaquark denoted as $P_c^+(4337)$ in the invariant mass spectrum of the $J/\psi p$ in the $B_s^0 \rightarrow J/\psi p \bar{p}$ decays [3]. On the other hand, the search for the LHCb pentaquarks $P_c^+(4312)$, $P_c^+(4440)$ and $P_c^+(4457)$ by the GlueX Collaboration in Hall D at JLab through a scan of the cross section of elastic reaction $\gamma p \rightarrow J/\psi p$ from threshold of 8.21 GeV and up to incident photon energy $E_\gamma = 11.8$ GeV gave no evidence for them with present statistics and set the model-dependent upper limits on branching ratios of $P_c^+(4312) \rightarrow J/\psi p$, $P_c^+(4440) \rightarrow J/\psi p$ and $P_c^+(4457) \rightarrow J/\psi p$ decays of several percent [4]. The preliminary results from a factor of 10 more data on the J/ψ photoproduction on a hydrogen target, collected in the Hall C JLab E12-16-007 experiment (the so-called J/ψ -007 experiment), also show no P_c^+ signal [5]. In this experiment the e^+e^- pairs from the J/ψ decays were detected in coincidence using the two high momentum spectrometers of Hall C: the Super High Momentum Spectrometer (SHMS) and High Momentum Spectrometer (HMS) for the electron and the positron, respectively. In recent publications [6] and [7] the role, respectively, of the LHCb pentaquarks $P_c^+(4450)$ and $P_c^+(4312)$, $P_c^+(4440)$, $P_c^+(4457)$ in charmonium photoproduction on protons and nuclei has been investigated at near-threshold initial photon energies $E_\gamma \leq 11$ GeV. Here, the description was based on the consideration of the incoherent direct ($\gamma N \rightarrow J/\psi N$) and two-step ($\gamma p \rightarrow P_c^+(4450) \rightarrow J/\psi p$ and $\gamma p \rightarrow P_c^+(4312) \rightarrow J/\psi p$, $\gamma p \rightarrow P_c^+(4440) \rightarrow J/\psi p$, $\gamma p \rightarrow P_c^+(4457) \rightarrow J/\psi p$) J/ψ production processes. As a measure for this role, the incident photon energy dependence of J/ψ production cross sections on protons and nuclei (excitation functions) has been adopted. It was found that it is insignificant for the pentaquark resonances considered if branching ratios of their decays to the $J/\psi p$ mode are less than a few percent, which is in line with the results of the JLab experiments [4, 5].

In view of the aforementioned, to get a robust enough information for or against the existence of the LHCb hidden-charm pentaquarks and to understand them better, it is crucial to investigate the possibility of their observation by measuring not only the excitation functions for J/ψ meson production from photon-induced reactions on protons and nuclei at near-threshold photon energies, predicted in Refs. [6, 7], but also the J/ψ energy and momentum distributions in these reactions, not predicted in the previous papers [6, 7]. Their prediction is the main aim of the present study. In it, we consider the contribution of the $P_c^{+,0}(4312)$, $P_c^{+,0}(4337)$, $P_c^{+,0}(4440)$ and $P_c^{+,0}(4457)$ resonances to near-threshold J/ψ photoproduction off protons and nuclei by adopting the Breit-Wigner shape for this contribution and by employing the recent experimental data [4] on the total and differential cross sections of the $\gamma p \rightarrow J/\psi p$ process to estimate the background contribution. The consideration is mainly based on the model, developed in Refs. [6, 7]. We present the predictions obtained within our present approach for the J/ψ energy and momentum distributions in γp as well as in $\gamma^{12}\text{C}$ and $\gamma^{184}\text{W}$ reactions at near-threshold incident photon energies. These predictions may be useful in planning future J/ψ photoproduction experiments at the CEBAF facility.

2. Theoretical framework

2.1. Direct non-resonant J/ψ production processes

At near-threshold photon beam energies below 11 GeV of our interest ¹⁾, the following direct non-resonant elementary charmonium production processes with the lowest free production threshold (≈ 8.21 GeV) contribute to the J/ψ photoproduction on nuclei [6–8]:

$$\gamma + p \rightarrow J/\psi + p, \quad (1)$$

$$\gamma + n \rightarrow J/\psi + n. \quad (2)$$

The modification of the masses of the final high-momentum J/ψ meson and proton (see below) in the nuclear medium will be ignored in the present study.

Disregarding the absorption of incident photons in the energy range of interest as well as the J/ψ meson quasielastic rescatterings on target nucleons [9], and describing the charmonium final-state absorption in the nuclear matter by the absorption cross section $\sigma_{J/\psi N}$ ²⁾, we represent the inclusive differential cross section for the production of J/ψ mesons with the momentum $\mathbf{p}_{J/\psi}$ on nuclei in the direct non-resonant processes (1), (2) in the form [6–10]:

$$\frac{d\sigma_{\gamma A \rightarrow J/\psi X}^{(\text{dir})}(\mathbf{p}_\gamma, \mathbf{p}_{J/\psi})}{d\mathbf{p}_{J/\psi}} = I_V[A, \sigma_{J/\psi N}] \left\langle \frac{d\sigma_{\gamma p \rightarrow J/\psi p}(\mathbf{p}_\gamma, \mathbf{p}_{J/\psi})}{d\mathbf{p}_{J/\psi}} \right\rangle_A, \quad (3)$$

where

$$I_V[A, \sigma] = 2\pi A \int_0^R r_\perp dr_\perp \int_{-\sqrt{R^2 - r_\perp^2}}^{\sqrt{R^2 - r_\perp^2}} dz \rho(\sqrt{r_\perp^2 + z^2}) \exp \left[-A\sigma \int_z^{\sqrt{R^2 - r_\perp^2}} \rho(\sqrt{r_\perp^2 + x^2}) dx \right], \quad (4)$$

$$\left\langle \frac{d\sigma_{\gamma p \rightarrow J/\psi p}(\mathbf{p}_\gamma, \mathbf{p}_{J/\psi})}{d\mathbf{p}_{J/\psi}} \right\rangle_A = \int \int P_A(\mathbf{p}_t, E) d\mathbf{p}_t dE \left[\frac{d\sigma_{\gamma p \rightarrow J/\psi p}(\sqrt{s^*}, \mathbf{p}_{J/\psi})}{d\mathbf{p}_{J/\psi}} \right] \quad (5)$$

and

$$s^* = (E_\gamma + E_t)^2 - (\mathbf{p}_\gamma + \mathbf{p}_t)^2, \quad (6)$$

$$E_t = M_A - \sqrt{(-\mathbf{p}_t)^2 + (M_A - m_p + E)^2}. \quad (7)$$

Here, $d\sigma_{\gamma p \rightarrow J/\psi p}(\sqrt{s^*}, \mathbf{p}_{J/\psi})/d\mathbf{p}_{J/\psi}$ is the off-shell differential cross section for the production of J/ψ meson in process (1) at the "in-medium" γp c.m. energy $\sqrt{s^*}$ ³⁾; $\rho(\mathbf{r})$ and $P_A(\mathbf{p}_t, E)$ are normalized to unity the nucleon density and the nuclear spectral function (they are given in Refs. [11, 12]) of target nucleus with mass number A , having mass M_A and radius R ; \mathbf{p}_γ and E_γ are the momentum and energy of the incident photon ($E_\gamma = |\mathbf{p}_\gamma| = p_\gamma$) in the laboratory system; \mathbf{p}_t and E are the momentum and binding energy of the intranuclear target proton, participating in the reaction channel (1); m_p is the free space proton mass.

¹⁾These energies are well within the present capabilities of the upgraded CEBAF facility at JLab, which is providing an opportunity to study the observed [1–3] by the LHCb Collaboration exotic hidden-charm pentaquark states in exclusive $\gamma p \rightarrow J/\psi p$ reactions in all experimental Halls A, B, C, D [4, 5].

²⁾For which we will use the value $\sigma_{J/\psi N} = 3.5$ mb [6–10].

³⁾In Eq. (3), it is assumed that the cross sections for J/ψ meson production in γp and γn interactions are equal to each other [6–8].

Also, as previously in [6–8], we will suppose that the off-shell differential cross section $d\sigma_{\gamma p \rightarrow J/\psi p}(\sqrt{s^*}, \mathbf{p}_{J/\psi})/d\mathbf{p}_{J/\psi}$ for J/ψ production in process (1) is the same as the corresponding on-shell cross section $d\sigma_{\gamma p \rightarrow J/\psi p}(\sqrt{s}, \mathbf{p}_{J/\psi})/d\mathbf{p}_{J/\psi}$ determined for the off-shell kinematics of this process and in which the vacuum c.m. energy squared s , given by the formula

$$s = W^2 = (E_\gamma + m_p)^2 - \mathbf{p}_\gamma^2 = m_p^2 + 2m_p E_\gamma, \quad (8)$$

is replaced by the in-medium expression (6). The above off-shell differential cross section is then (cf. [8, 10]):

$$\begin{aligned} \frac{d\sigma_{\gamma p \rightarrow J/\psi p}(\sqrt{s^*}, \mathbf{p}_{J/\psi})}{d\mathbf{p}_{J/\psi}} &= \frac{\pi}{I_2(s^*, m_{J/\psi}, m_p) E_{J/\psi}} \\ &\times \frac{d\sigma_{\gamma p \rightarrow J/\psi p}(\sqrt{s^*}, \theta_{J/\psi}^*)}{d\Omega_{J/\psi}^*} \frac{1}{(\omega + E_t)} \delta \left[\omega + E_t - \sqrt{m_p^2 + (\mathbf{Q} + \mathbf{p}_t)^2} \right], \end{aligned} \quad (9)$$

where

$$I_2(s^*, m_{J/\psi}, m_p) = \frac{\pi}{2} \frac{\lambda(s^*, m_{J/\psi}^2, m_p^2)}{s^*}, \quad (10)$$

$$\lambda(x, y, z) = \sqrt{[x - (\sqrt{y} + \sqrt{z})^2][x - (\sqrt{y} - \sqrt{z})^2]}, \quad (11)$$

$$\omega = E_\gamma - E_{J/\psi}, \quad \mathbf{Q} = \mathbf{p}_\gamma - \mathbf{p}_{J/\psi}, \quad E_{J/\psi} = \sqrt{m_{J/\psi}^2 + \mathbf{p}_{J/\psi}^2}. \quad (12)$$

Here, the off-shell c.m. charmonium angular distribution in reaction (1) $d\sigma_{\gamma p \rightarrow J/\psi p}(\sqrt{s^*}, \theta_{J/\psi}^*)/d\Omega_{J/\psi}^*$ as a function of the J/ψ production c.m. polar angle $\theta_{J/\psi}^*$ is given by [10]:

$$\frac{d\sigma_{\gamma p \rightarrow J/\psi p}(\sqrt{s^*}, \theta_{J/\psi}^*)}{d\Omega_{J/\psi}^*} = a e^{b_{J/\psi}(t-t^+)} \sigma_{\gamma p \rightarrow J/\psi p}(\sqrt{s^*}), \quad (13)$$

where $\sigma_{\gamma p \rightarrow J/\psi p}(\sqrt{s^*})$ is the off-shell total cross section for J/ψ meson production in this reaction and

$$t = m_{J/\psi}^2 - 2E_\gamma^* E_{J/\psi}^* + 2p_\gamma^* p_{J/\psi}^* \cos \theta_{J/\psi}^*, \quad (14)$$

$$E_\gamma^* = p_\gamma^*, \quad E_{J/\psi}^* = \sqrt{m_{J/\psi}^2 + p_{J/\psi}^{*2}}, \quad (15)$$

$$p_\gamma^* = \frac{1}{2\sqrt{s^*}} \lambda(s^*, 0, E_t^2 - p_t^2), \quad (16)$$

$$p_{J/\psi}^* = \frac{1}{2\sqrt{s^*}} \lambda(s^*, m_{J/\psi}^2, m_p^2), \quad (17)$$

$$t^+ = t(\cos \theta_{J/\psi}^* = 1) = m_{J/\psi}^2 - 2E_\gamma^* E_{J/\psi}^* + 2p_\gamma^* p_{J/\psi}^*, \quad (18)$$

$$t - t^+ = 2p_\gamma^* p_{J/\psi}^* (\cos \theta_{J/\psi}^* - 1). \quad (19)$$

The angle of charmonium production in the γp c.m. system, $\theta_{J/\psi}^*$, is expressed through its production angle, $\theta_{J/\psi}$, in the laboratory system ($\cos \theta_{J/\psi} = \mathbf{p}_\gamma \mathbf{p}_{J/\psi} / p_\gamma p_{J/\psi}$) by means of equation [8, 10]:

$$\cos \theta_{J/\psi}^* = \frac{p_\gamma p_{J/\psi} \cos \theta_{J/\psi} + (E_\gamma^* E_{J/\psi}^* - E_\gamma E_{J/\psi})}{p_\gamma^* p_{J/\psi}^*}. \quad (20)$$

The condition of normalization

$$\int_{4\pi} a e^{b_{J/\psi}(t-t^+)} d\Omega_{J/\psi}^* = 1 \quad (21)$$

gives for the parameter a in Eq. (13) the following expression:

$$a = \frac{p_{\gamma}^* p_{J/\psi}^* b_{J/\psi}}{\pi} \left[1 - e^{-4p_{\gamma}^* p_{J/\psi}^* b_{J/\psi}} \right]^{-1}. \quad (22)$$

Parameter $b_{J/\psi}$ in Eqs. (13), (21), (22) is an exponential t -slope of the differential cross section of the reaction $\gamma p \rightarrow J/\psi p$ in the near-threshold energy region. It should be pointed out that the differential cross section of this reaction was also very recently measured in the J/ψ -007 experiment [13] as a function of the photon energy in the range of $9.1 \text{ GeV} \leq E_{\gamma} \leq 10.6 \text{ GeV}$ with the aim to explore the impact of the collected data on the determination of the proton's gravitational form factors, the proton-mass radius, and the contribution of the trace anomaly to the proton mass. Since the t -slope $b_{J/\psi}$ was not determined in [13], we will adopt for it the GlueX result [4], namely: $b_{J/\psi} \approx 1.67 \text{ GeV}^{-2}$. We will use this value in our calculations.

Now consider the off-shell total cross section $\sigma_{\gamma p \rightarrow J/\psi p}(\sqrt{s^*})$ for J/ψ production in process (1). In line with the above-mentioned, it is the same as the vacuum cross section $\sigma_{\gamma p \rightarrow J/\psi p}(\sqrt{s})$, in which the vacuum c.m. energy squared s , defined by the formula (8), is replaced by the in-medium expression (6). For the vacuum total cross section $\sigma_{\gamma p \rightarrow J/\psi p}(\sqrt{s})$ at near-threshold photon energies we have used the following parametrization [7] of the available here experimental information [4] on it from the GlueX experiment, based on the near-threshold predictions of the two gluon and three gluon exchange model [14]:

$$\sigma_{\gamma p \rightarrow J/\psi p}(\sqrt{s}) = \sigma_{2g}(\sqrt{s}) + \sigma_{3g}(\sqrt{s}), \quad (23)$$

where $2g$ and $3g$ exchanges cross sections $\sigma_{2g}(\sqrt{s})$ and $\sigma_{3g}(\sqrt{s})$ are given in Ref. [7] by formulas (7) and (8), respectively. Fig. 1 shows that the GlueX near-threshold data are well fitted by only the combination (23) of the two gluon and three gluon exchange cross sections and in the resonance incident photon energy range $\sim 9.5\text{--}10.0 \text{ GeV}$ the main contribution to the elastic J/ψ production comes from the three gluon exchanges.

At the initial photon energies of interest the J/ψ mesons are produced at small laboratory polar angles (see below). Therefore, we will calculate the J/ψ momentum distributions from considered target nuclei for the laboratory solid angle $\Delta\Omega_{J/\psi}=0^\circ \leq \theta_{J/\psi} \leq 20^\circ$, and $0 \leq \varphi_{J/\psi} \leq 2\pi$ (cf. [10]). Then, integrating the differential cross section (3) over this solid angle, we can represent the differential cross section for charmonium production from the direct non-resonant processes (1) and (2) into this solid angle as follows:

$$\begin{aligned} \frac{d\sigma_{\gamma A \rightarrow J/\psi X}^{(\text{dir})}(p_{\gamma}, p_{J/\psi})}{dp_{J/\psi}} &= \int_{\Delta\Omega_{J/\psi}} d\Omega_{J/\psi} \frac{d\sigma_{\gamma A \rightarrow J/\psi X}^{(\text{dir})}(\mathbf{p}_{\gamma}, \mathbf{p}_{J/\psi})}{d\mathbf{p}_{J/\psi}} p_{J/\psi}^2 \\ &= 2\pi I_V[A, \sigma_{J/\psi N}] \int_{\cos 20^\circ}^1 d\cos\theta_{J/\psi} \left\langle \frac{d\sigma_{\gamma p \rightarrow J/\psi p}(p_{\gamma}, p_{J/\psi}, \theta_{J/\psi})}{dp_{J/\psi} d\Omega_{J/\psi}} \right\rangle_A. \end{aligned} \quad (24)$$

Before going further, we now consider, adopting the relativistic kinematics, more simpler case of the free space production of J/ψ mesons and protons in the process $\gamma p \rightarrow J/\psi p$, proceeding on a free target proton being at rest, to get an idea about their kinematic characteristics allowed in this process at incident photon energies considered. The kinematics of two-body reaction with a threshold (as in our present case) tell us that the laboratory polar J/ψ and final proton production angles $\theta_{J/\psi}$ and θ_p vary from 0 to a maximal values $\theta_{J/\psi}^{\text{max}}$ and θ_p^{max} , correspondingly, i.e.:

$$0 \leq \theta_{J/\psi} \leq \theta_{J/\psi}^{\text{max}}, \quad (25)$$

$$0 \leq \theta_p \leq \theta_p^{\text{max}}; \quad (26)$$

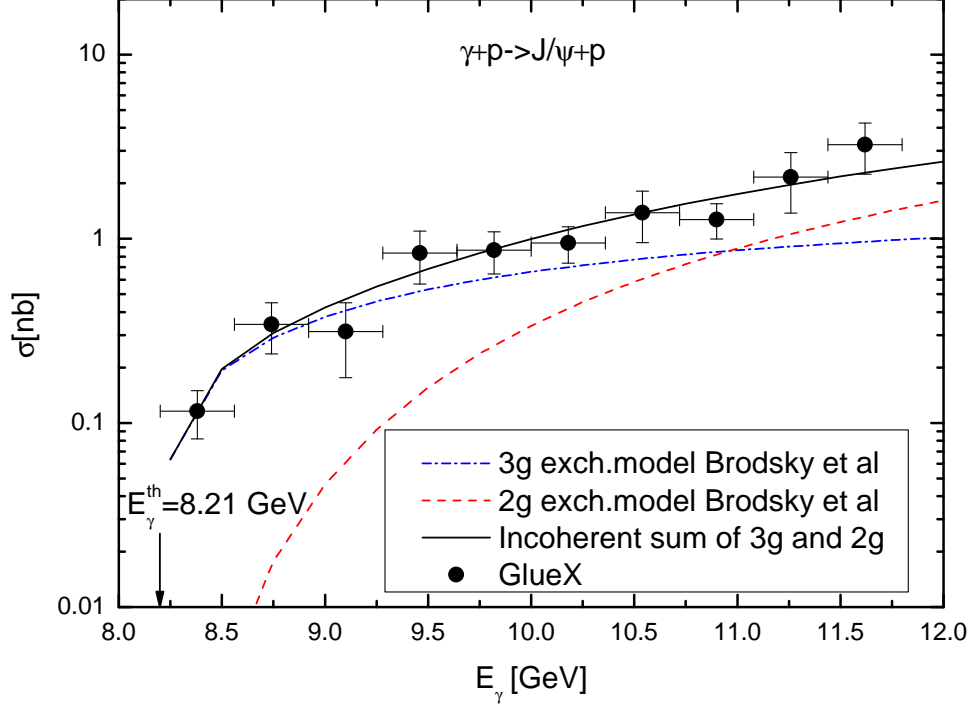


Figure 1: (Color online) The total cross section for the background reaction $\gamma p \rightarrow J/\psi p$ as a function of the photon energy E_γ . Dashed and dotted-dashed curves are, respectively, calculations on the basis of the two gluon and three gluon exchange model [14]. Solid curve is the incoherent sum of the above two calculations. The GlueX experimental data are from Ref. [4]. The arrow indicates the threshold energy of 8.21 GeV for direct non-resonant charmonium photoproduction off a free target proton at rest.

where

$$\theta_{J/\psi}^{\max} = \arcsin[(\sqrt{s} p_{J/\psi}^*) / (m_{J/\psi} p_\gamma)], \quad (27)$$

$$\theta_p^{\max} = \arcsin[(\sqrt{s} p_p^*) / (m_p p_\gamma)]. \quad (28)$$

Here, the J/ψ c.m. momentum $p_{J/\psi}^*$ is determined by Eq. (17), in which the in-medium c.m. energy squared s^* should be replaced by the vacuum collision energy squared s , defined by the formula (8), and p_p^* is the final proton c.m. momentum. It is equal to the J/ψ c.m. momentum $p_{J/\psi}^*$. From Eqs. (27), (28) one can get, for example, that

$$\theta_{J/\psi}^{\max} = 5.570^\circ, \quad \theta_p^{\max} = 18.686^\circ \quad (29)$$

at initial photon beam energy of $E_\gamma = 9.44$ GeV and

$$\theta_{J/\psi}^{\max} = 6.768^\circ, \quad \theta_p^{\max} = 22.892^\circ \quad (30)$$

at photon energy of $E_\gamma = 10.12$ GeV. Energy-momentum conservation in the reaction (1), taking place in a vacuum, leads to two different solutions for the laboratory J/ψ meson and final proton momenta $p_{J/\psi}$ and p_p at given laboratory polar production angles $\theta_{J/\psi}$ and θ_p , belonging, correspondingly, to the angular intervals (25) and (26):

$$p_{J/\psi}^{(1,2)}(\theta_{J/\psi}) = \frac{p_\gamma \sqrt{s} E_{J/\psi}^* \cos \theta_{J/\psi} \pm (E_\gamma + m_p) \sqrt{s} \sqrt{p_{J/\psi}^{*2} - \gamma_{\text{cm}}^2 v_{\text{cm}}^2 m_{J/\psi}^2 \sin^2 \theta_{J/\psi}}}{(E_\gamma + m_p)^2 - p_\gamma^2 \cos^2 \theta_{J/\psi}}, \quad (31)$$

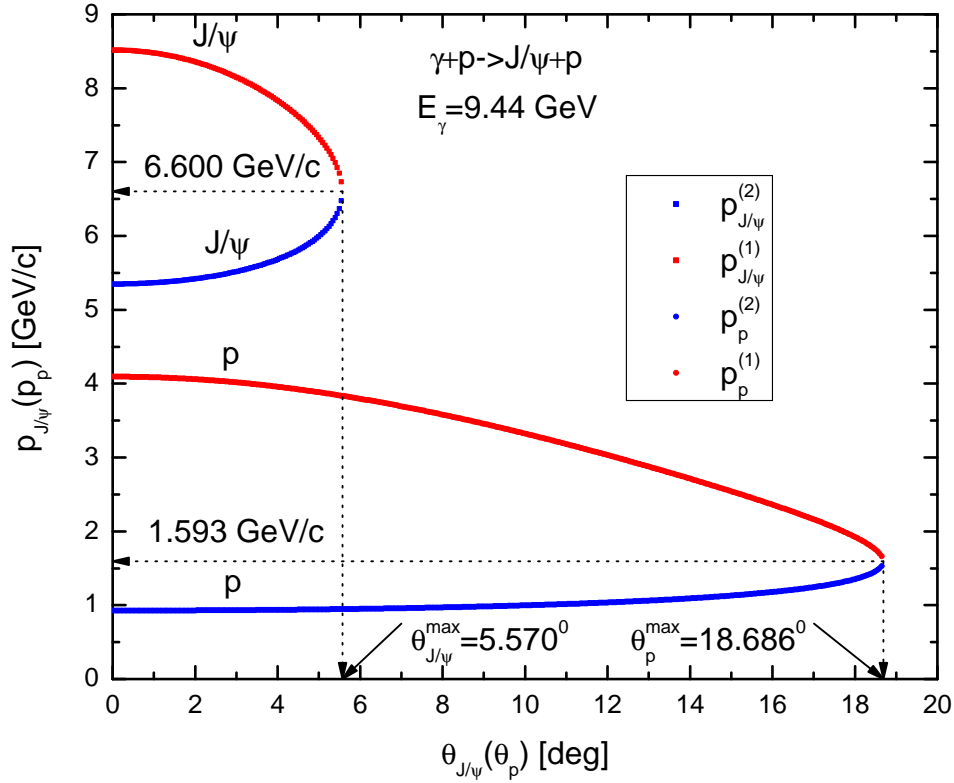


Figure 2: (Color online) Plot of the allowed final J/ψ meson and proton momenta in the direct non-resonant $\gamma p \rightarrow J/\psi p$ reaction, occurring in the laboratory system in the free space at initial photon energy of 9.44 GeV, as functions of their production angles with respect to the photon beam direction in this system.

$$p_p^{(1,2)}(\theta_p) = \frac{p_\gamma \sqrt{s} E_p^* \cos \theta_p \pm (E_\gamma + m_p) \sqrt{s} \sqrt{p_p^{*2} - \gamma_{\text{cm}}^2 v_{\text{cm}}^2 m_p^2 \sin^2 \theta_p}}{(E_\gamma + m_p)^2 - p_\gamma^2 \cos^2 \theta_p}. \quad (32)$$

Here, $\gamma_{\text{cm}} = (E_\gamma + m_p)/\sqrt{s}$, $v_{\text{cm}} = p_\gamma/(E_\gamma + m_p)$, the J/ψ total c.m. energy $E_{J/\psi}^*$ is defined above by Eq. (15), $E_p^* = \sqrt{m_p^2 + p_p^{*2}}$ and sign "+" in the numerators of Eqs. (31), (32) corresponds to the first solutions $p_{J/\psi}^{(1)}$, $p_p^{(1)}$ and sign "-" - to the second ones $p_{J/\psi}^{(2)}$, $p_p^{(2)}$. Looking at the expressions (31) and (32), one can come to the conclusion that the first solutions $p_{J/\psi}^{(1)}$ and $p_p^{(1)}$ as well as the second ones $p_{J/\psi}^{(2)}$ and $p_p^{(2)}$ have different dependencies, respectively, on the production angles $\theta_{J/\psi}$ and θ_p within the angular intervals $[0, \theta_{J/\psi}^{\text{max}}]$ and $[0, \theta_p^{\text{max}}]$. Namely, the former drop and the latter ones increase as the production angles $\theta_{J/\psi}$ and θ_p increase in these intervals (cf. Figs. 2 and 3) and

$$p_{J/\psi}^{(1)}(\theta_{J/\psi}^{\text{max}}) = p_{J/\psi}^{(2)}(\theta_{J/\psi}^{\text{max}}) = p_{J/\psi}(\theta_{J/\psi}^{\text{max}}), \quad (33)$$

$$p_p^{(1)}(\theta_p^{\text{max}}) = p_p^{(2)}(\theta_p^{\text{max}}) = p_p(\theta_p^{\text{max}}), \quad (34)$$

where

$$p_{J/\psi}(\theta_{J/\psi}^{\text{max}}) = (p_\gamma m_{J/\psi}^2 \cos \theta_{J/\psi}^{\text{max}})/(\sqrt{s} E_{J/\psi}^*), \quad (35)$$

$$p_p(\theta_p^{\text{max}}) = (p_\gamma m_p^2 \cos \theta_p^{\text{max}})/(\sqrt{s} E_p^*). \quad (36)$$

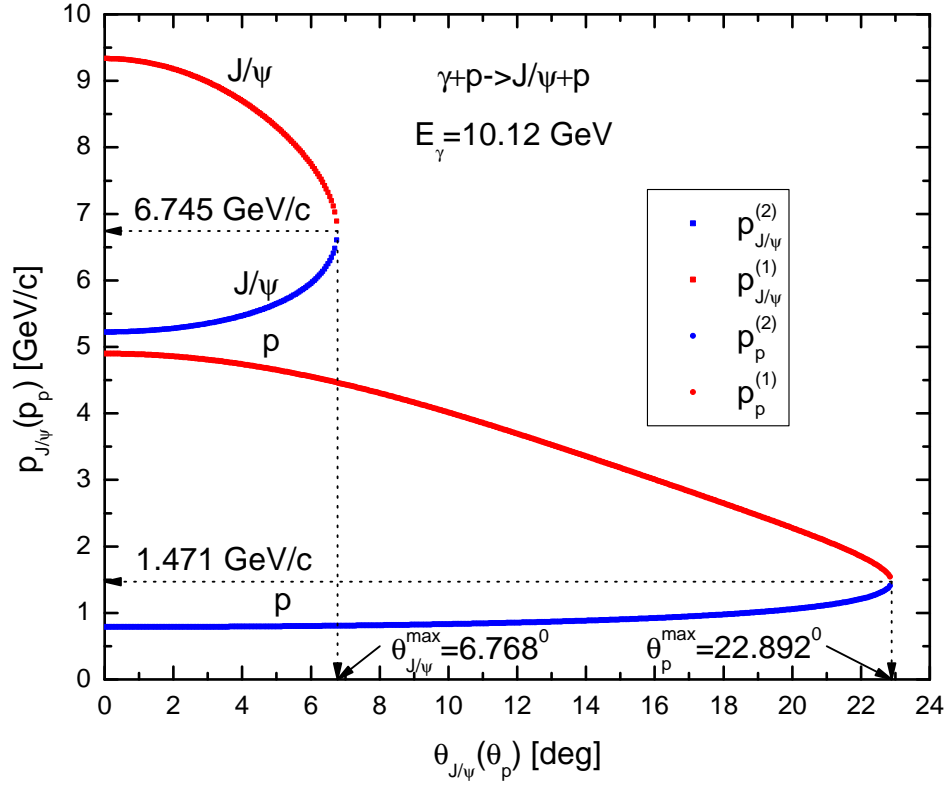


Figure 3: (Color online) The same as in Fig. 2, but for the initial photon energy of 10.12 GeV.

According to Eqs. (35), (36), for $E_\gamma = 9.44$ GeV we get then that $p_{J/\psi}(\theta_{J/\psi}^{\max}) = 6.600$ GeV/c and $p_p(\theta_p^{\max}) = 1.593$ GeV/c. For $E_\gamma = 10.12$ GeV we obtain $p_{J/\psi}(\theta_{J/\psi}^{\max}) = 6.745$ GeV/c and $p_p(\theta_p^{\max}) = 1.471$ GeV/c (cf. Figs. 2 and 3). These figures show that the kinematically allowed charmonium laboratory momenta and total energies in the direct non-resonant $\gamma p \rightarrow J/\psi p$ process, taking place on the free target proton at rest, at given initial photon energy vary within the following momentum and energy ranges:

$$p_{J/\psi}^{(2)}(0^\circ) \leq p_{J/\psi} \leq p_{J/\psi}^{(1)}(0^\circ), \quad (37)$$

$$E_{J/\psi}^{(2)}(0^\circ) \leq E_{J/\psi} \leq E_{J/\psi}^{(1)}(0^\circ), \quad (38)$$

where the quantities $p_{J/\psi}^{(1,2)}(0^\circ)$ are defined above by Eq. (31) and $E_{J/\psi}^{(1,2)}(0^\circ) = \sqrt{m_{J/\psi}^2 + [p_{J/\psi}^{(1,2)}(0^\circ)]^2}$.

Finally, we calculate the J/ψ energy distribution $d\sigma_{\gamma p \rightarrow J/\psi p}[\sqrt{s}, p_{J/\psi}]/dE_{J/\psi}$ from the reaction $\gamma p \rightarrow J/\psi p$ within the kinematically allowed interval (38). Integration of the more general differential cross section (9) over the angle $\theta_{J/\psi}$, when this angle varies in the allowed angular region (25), in the limits: $\mathbf{p}_t \rightarrow 0$, $E_t \rightarrow m_p$ and $s^* \rightarrow s$ yields:

$$\begin{aligned} \frac{d\sigma_{\gamma p \rightarrow J/\psi p}[\sqrt{s}, p_{J/\psi}]}{dE_{J/\psi}} &= 2\pi \int_{\cos \theta_{J/\psi}^{\max}}^1 d\cos \theta_{J/\psi} p_{J/\psi} E_{J/\psi} \frac{d\sigma_{\gamma p \rightarrow J/\psi p}[\sqrt{s}, \mathbf{p}_{J/\psi}]}{d\mathbf{p}_{J/\psi}} = \\ &= \left(\frac{2\pi\sqrt{s}}{p_\gamma p_{J/\psi}^*} \right) \frac{d\sigma_{\gamma p \rightarrow J/\psi p}[\sqrt{s}, \theta_{J/\psi}^*(x_0)]}{d\Omega_{J/\psi}^*} \text{ for } E_{J/\psi}^{(2)}(0^\circ) \leq E_{J/\psi} \leq E_{J/\psi}^{(1)}(0^\circ), \end{aligned} \quad (39)$$

where

$$x_0 = \frac{[p_\gamma^2 + p_{J/\psi}^2 + m_p^2 - (\omega + m_p)^2]}{2p_\gamma p_{J/\psi}}, \quad p_{J/\psi} = \sqrt{E_{J/\psi}^2 - m_{J/\psi}^2} \quad (40)$$

and the quantity $\cos \theta_{J/\psi}^*(x_0)$ is defined by Eq. (20), in which one has to perform the replacement: $\cos \theta_{J/\psi} \rightarrow x_0$, and the photon and J/ψ c.m. momenta p_γ^* and $p_{J/\psi}^*$ are defined by formulas (16) and (17), correspondingly, in which one needs also to make the substitutions: $E_t \rightarrow m_p$, $p_t \rightarrow 0$ and $s^* \rightarrow s$. We will adopt the expression (39) for evaluating the free space J/ψ energy distribution from the direct process (1), proceeding on a proton at rest, for incident photon beam resonant energies of 9.44, 9.554, 10.04 and 10.12 GeV (see below).

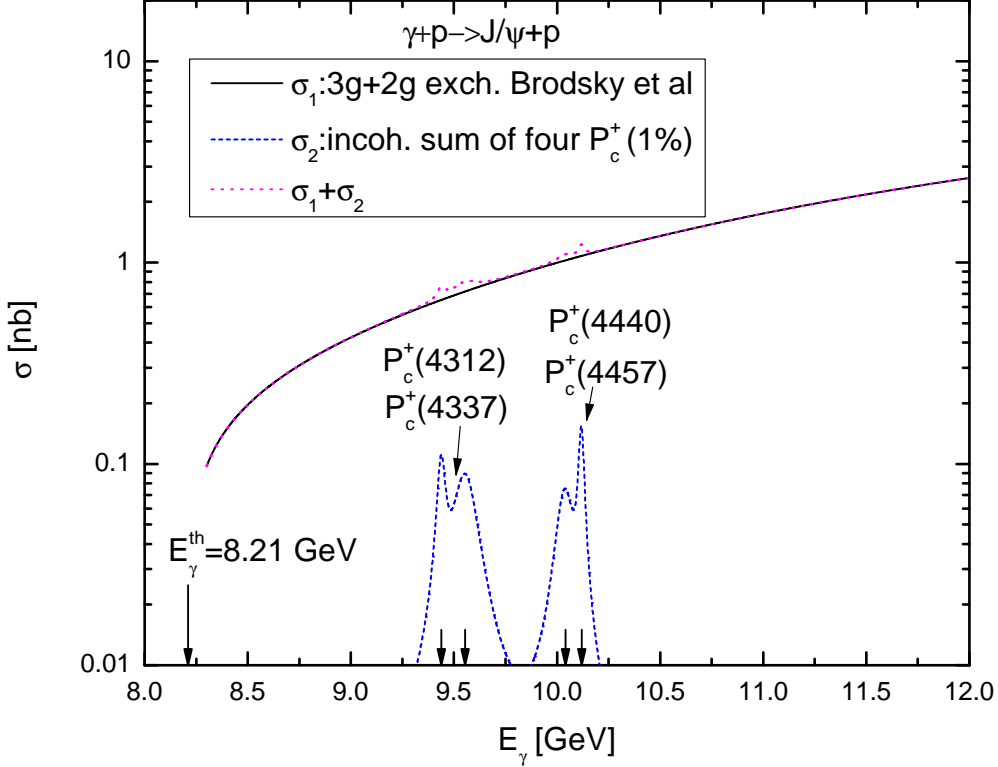


Figure 4: (Color online) The non-resonant total cross section σ_1 for the reaction $\gamma p \rightarrow J/\psi p$ (solid curve) and the incoherent sum (dotted curve) of it and the total cross section σ_2 (short-dashed curve) for the resonant J/ψ production in the processes $\gamma p \rightarrow P_c^+(4312) \rightarrow J/\psi p$, $\gamma p \rightarrow P_c^+(4337) \rightarrow J/\psi p$, $\gamma p \rightarrow P_c^+(4440) \rightarrow J/\psi p$ and $\gamma p \rightarrow P_c^+(4457) \rightarrow J/\psi p$, calculated assuming that the resonances $P_c^+(4312)$, $P_c^+(4337)$, $P_c^+(4440)$ and $P_c^+(4457)$ with the spin-parity quantum numbers $J^P = (1/2)^-$, $J^P = (1/2)^-$, $J^P = (1/2)^-$ and $J^P = (3/2)^-$ decay to $J/\psi p$ with the lower allowed relative orbital angular momentum $L = 0$ with all four branching fractions $Br[P_{ci}^+ \rightarrow J/\psi p] = 1\%$, as functions of photon energy. The left and four right arrows indicate, correspondingly, the threshold energy $E_\gamma^{\text{th}} = 8.21$ GeV for the reaction $\gamma p \rightarrow J/\psi p$ proceeding on a free target proton being at rest and the resonant energies $E_\gamma^{\text{R1}} = 9.44$ GeV, $E_\gamma^{\text{R2}} = 9.554$ GeV, $E_\gamma^{\text{R3}} = 10.04$ GeV and $E_\gamma^{\text{R4}} = 10.12$ GeV.

2.2. Two-step resonant J/ψ production processes

At photon energies below 11 GeV, incident photons can produce the observed [1–3] experimentally non-strange charged $P_c^+(4312)$, $P_c^+(4337)$, $P_c^+(4440)$, $P_c^+(4457)$ pentaquark resonances with quark structure $|P_c^+ \rangle = |uudc\bar{c}\rangle$ and predicted [15], but non-observed yet their neutral isospin partners $P_c^0(4312)$, $P_c^0(4337)$, $P_c^0(4440)$, $P_c^0(4457)$ ⁴⁾ directly in the first inelastic collisions with intranuclear protons and neutrons⁵⁾:

$$\begin{aligned}\gamma + p &\rightarrow P_c^+(4312), \\ \gamma + p &\rightarrow P_c^+(4337), \\ \gamma + p &\rightarrow P_c^+(4440), \\ \gamma + p &\rightarrow P_c^+(4457);\end{aligned}\tag{41}$$

$$\begin{aligned}\gamma + n &\rightarrow P_c^0(4312), \\ \gamma + n &\rightarrow P_c^0(4337), \\ \gamma + n &\rightarrow P_c^0(4440), \\ \gamma + n &\rightarrow P_c^0(4457).\end{aligned}\tag{42}$$

Furthermore, the produced pentaquark resonances can decay into the final states $J/\psi p$ and $J/\psi n$, which will additionally contribute to the J/ψ yield in the $(\gamma, J/\psi)$ reactions on protons and nuclei:

$$\begin{aligned}P_c^+(4312) &\rightarrow J/\psi + p, \\ P_c^+(4337) &\rightarrow J/\psi + p, \\ P_c^+(4440) &\rightarrow J/\psi + p, \\ P_c^+(4457) &\rightarrow J/\psi + p;\end{aligned}\tag{43}$$

$$\begin{aligned}P_c^0(4312) &\rightarrow J/\psi + n, \\ P_c^0(4337) &\rightarrow J/\psi + n, \\ P_c^0(4440) &\rightarrow J/\psi + n, \\ P_c^0(4457) &\rightarrow J/\psi + n.\end{aligned}\tag{44}$$

The branching ratios $Br[P_{ci}^+ \rightarrow J/\psi p]$ ⁶⁾ of the decays (43) have not been determined yet. Model-dependent upper limits on branching fractions $Br[P_c^+(4312) \rightarrow J/\psi p]$, $Br[P_c^+(4440) \rightarrow J/\psi p]$ and $Br[P_c^+(4457) \rightarrow J/\psi p]$ of several percent were set by the GlueX Hall-D experiment [4] at JLab, having a moderate statistics (about 470 J/ψ events). Preliminary results from a factor of 10 more data (about 4000 J/ψ events), collected in the J/ψ -007 Hall-C experiment [17] at JLab as well, focused on the large t region⁷⁾ in searching for the LHCb hidden-charm pentaquarks [1, 2],

⁴⁾The minimal quark content of the P_c^0 states is $|P_c^0 \rangle = |uddc\bar{c}\rangle$. Following the observation of the narrow pentaquarks $P_c^+(4312)$, $P_c^+(4440)$ and $P_c^+(4457)$ by the LHCb Collaboration [1, 2], it was proposed to search for the P_c^0 states in $\pi^- p \rightarrow J/\psi n$ reaction [16].

⁵⁾We remind that, for example, the threshold (resonant) energies E_γ^{R1} , E_γ^{R2} , E_γ^{R3} and E_γ^{R4} for the photoproduction of the P_c^+ resonances with pole masses $M_{c1}^+ = 4311.9$ MeV, $M_{c2}^+ = 4337.0$ MeV, $M_{c3}^+ = 4440.3$ MeV and $M_{c4}^+ = 4457.3$ MeV [2, 3] on a free target proton being at rest are $E_\gamma^{R1} = 9.44$ GeV, $E_\gamma^{R2} = 9.554$ GeV, $E_\gamma^{R3} = 10.04$ GeV and $E_\gamma^{R4} = 10.12$ GeV, respectively.

⁶⁾Here, $i = 1, 2, 3, 4$ and P_{c1}^+ , P_{c2}^+ , P_{c3}^+ and P_{c4}^+ stand for $P_c^+(4312)$, $P_c^+(4337)$, $P_c^+(4440)$ and $P_c^+(4457)$, respectively. Analogously, P_{c1}^0 , P_{c2}^0 , P_{c3}^0 and P_{c4}^0 will denote below the $P_c^0(4312)$, $P_c^0(4337)$, $P_c^0(4440)$ and $P_c^0(4457)$ states.

⁷⁾In which the rather flat resonant production of J/ψ through the P_c^+ is expected to be enhanced relative to the suppressed here mostly forward diffractive production.

also observe no signals for them and will set more stringent upper limits on the above branching fractions and on pentaquark- J/ψ couplings. Based on the branching ratios and fractions measured by the LHCb and GlueX Collaborations, the authors of Ref. [18] obtain that a lower limit of $Br[P_c^+ \rightarrow J/\psi p]$ is of the order of $0.05\% \sim 0.5\%$. Taking into account these findings, we will adopt in our study for the four branching ratios $Br[P_{ci}^+ \rightarrow J/\psi p]$ of the decays (43) three following conservative options: $Br[P_{ci}^+ \rightarrow J/\psi p] = 0.25, 0.5$ and 1% ($i = 1, 2, 3, 4$), and in line with Ref. [15], will assume that $Br[P_{ci}^0 \rightarrow J/\psi n] = Br[P_{ci}^+ \rightarrow J/\psi p]$. This will allow us to get a better impression of the size of the effect of branching fractions $Br[P_{ci}^+ \rightarrow J/\psi p]$ and $Br[P_{ci}^0 \rightarrow J/\psi n]$ on the resonant J/ψ yield in $\gamma p \rightarrow J/\psi p$ as well as in $\gamma^{12}\text{C} \rightarrow J/\psi X$ and $\gamma^{184}\text{W} \rightarrow J/\psi X$ reactions. Moreover, we will also suppose, analogously to [15], for the P_{ci}^0 states the same pole masses M_{ci}^0 and total decay width Γ_{ci}^0 as those M_{ci}^+ and Γ_{ci}^+ for their hidden-charm charged counterparts P_{ci}^+ , i.e.: $M_{ci}^0 = M_{ci}^+$ and $\Gamma_{c1}^0 = \Gamma_{c1}^+ = 9.8$ MeV, $\Gamma_{c2}^0 = \Gamma_{c2}^+ = 29.0$ MeV, $\Gamma_{c3}^0 = \Gamma_{c3}^+ = 20.6$ MeV, $\Gamma_{c4}^0 = \Gamma_{c4}^+ = 6.4$ MeV [2, 3].

In line with Refs. [6, 7, 19], we suppose that the in-medium spectral functions $S_{ci}^+(\sqrt{s^*}, \Gamma_{ci}^+)$ and $S_{ci}^0(\sqrt{s^*}, \Gamma_{ci}^0)$ of the intermediate P_{ci}^+ and P_{ci}^0 resonances are described by the non-relativistic Breit-Wigner distributions ⁸⁾ :

$$S_{ci}^+(\sqrt{s^*}, \Gamma_{ci}^+) = \frac{1}{2\pi} \frac{\Gamma_{ci}^+}{(\sqrt{s^*} - M_{ci}^+)^2 + (\Gamma_{ci}^+)^2/4} \quad (45)$$

and

$$S_{ci}^0(\sqrt{s^*}, \Gamma_{ci}^0) = \frac{1}{2\pi} \frac{\Gamma_{ci}^0}{(\sqrt{s^*} - M_{ci}^0)^2 + (\Gamma_{ci}^0)^2/4}. \quad (46)$$

The in-medium total cross sections for production of these resonances with the possible spin-parity quantum numbers $J^P = (1/2)^-$ for P_{c1}^+ and P_{c1}^0 , $J^P = (1/2)^-$ for P_{c2}^+ and P_{c2}^0 , $J^P = (1/2)^-$ for P_{c3}^+ and P_{c3}^0 , and $J^P = (3/2)^-$ for P_{c4}^+ and P_{c4}^0 ⁹⁾ in reactions (41), (42) can be determined, using the spectral functions (45), (46) and known branching fractions $Br[P_{ci}^+ \rightarrow \gamma p]$ and $Br[P_{ci}^0 \rightarrow \gamma n]$ ($i = 1, 2, 3, 4$), as follows [6, 7, 19]:

$$\sigma_{\gamma p \rightarrow P_{ci}^+}(\sqrt{s^*}, \Gamma_{ci}^+) = f_{ci} \left(\frac{\pi}{p_\gamma^*} \right)^2 Br[P_{ci}^+ \rightarrow \gamma p] S_{ci}^+(\sqrt{s^*}, \Gamma_{ci}^+) \Gamma_{ci}^+, \quad i = 1, 2, 3, 4 \quad (47)$$

and

$$\sigma_{\gamma n \rightarrow P_{ci}^0}(\sqrt{s^*}, \Gamma_{ci}^0) = f_{ci} \left(\frac{\pi}{p_\gamma^*} \right)^2 Br[P_{ci}^0 \rightarrow \gamma n] S_{ci}^0(\sqrt{s^*}, \Gamma_{ci}^0) \Gamma_{ci}^0, \quad i = 1, 2, 3, 4. \quad (48)$$

Here, the c.m. 3-momentum in the incoming γN channel, p_γ^* , is defined above by Eq. (16) ¹⁰⁾ and the ratios of the spin factors $f_{c1} = 1$, $f_{c2} = 1$, $f_{c3} = 1$, $f_{c4} = 2$. Since we are mainly interested in the resonance P_c region, which is not far from the $J/\psi N$ production threshold, we suppose in line with [7, 19, 23] that the hidden-charm pentaquarks P_{ci}^+ and P_{ci}^0 decays to $J/\psi p$ and $J/\psi n$ modes are dominated by the lowest partial waves with zero relative orbital angular momentum L . In this case, adopting the vector-meson dominance model, one can obtain that the branching ratios $Br[P_{ci}^0 \rightarrow \gamma n]$ and $Br[P_{ci}^+ \rightarrow \gamma p]$ are equal to each other (cf. [24])

$$Br[P_{ci}^0 \rightarrow \gamma n] = Br[P_{ci}^+ \rightarrow \gamma p] \quad (49)$$

⁸⁾We ignore, for reasons of the simplification of calculations, the modification of the P_{ci}^+ and P_{ci}^0 masses and total decay widths in the nuclear matter in our present study.

⁹⁾Which might be assigned to them within the hadronic molecular scenario for their internal structure (cf. [7, 15, 20–22]).

¹⁰⁾For simplicity, we assume that the neutron mass m_n is equal to the proton mass m_p .

and the latter for $P_c^+(4312)$, $P_c^+(4440)$ and $P_c^+(4457)$ are expressed in the framework of this model via the branching fractions $Br[P_c^+(4312) \rightarrow J/\psi p]$, $Br[P_c^+(4440) \rightarrow J/\psi p]$ and $Br[P_c^+(4457) \rightarrow J/\psi p]$ by formula (24) from Ref. [7] and within this model we get that

$$Br[P_c^+(4337) \rightarrow \gamma p] = 1.48 \cdot 10^{-3} Br[P_c^+(4337) \rightarrow J/\psi p]. \quad (50)$$

Using Eqs. (47)–(49), we have

$$\sigma_{\gamma p \rightarrow P_{ci}^+}(\sqrt{s^*}, \Gamma_{ci}^+) = \sigma_{\gamma n \rightarrow P_{ci}^0}(\sqrt{s^*}, \Gamma_{ci}^0). \quad (51)$$

According to Eq. (47), for example, the free total cross sections $\sigma_{\gamma p \rightarrow P_{ci}^+ \rightarrow J/\psi p}(\sqrt{s}, \Gamma_{ci}^+)$ for resonant charmonium production in the two-step processes (41)/(43), taking place on the target proton at rest, can be represented as follows [6, 7]:

$$\sigma_{\gamma p \rightarrow P_{ci}^+ \rightarrow J/\psi p}(\sqrt{s}, \Gamma_{ci}^+) = \sigma_{\gamma p \rightarrow P_{ci}^+}(\sqrt{s}, \Gamma_{ci}^+) \theta[\sqrt{s} - (m_{J/\psi} + m_p)] Br[P_{ci}^+ \rightarrow J/\psi p]. \quad (52)$$

Here, $\theta(x)$ is the step function and the c.m. 3-momentum in the incoming γp channel, p_γ^* , entering into Eq. (47), is determined above by the formula (16), in which one has to make the replacements $E_t^2 - p_t^2 \rightarrow m_p^2$ and $s^* \rightarrow s$. In line with Eqs. (47) and (50), we see that these cross sections are proportional to $Br^2[P_{ci}^+ \rightarrow J/\psi p]$. This fact enables us to evaluate upper limits on the branching fractions $Br[P_c^+(4312) \rightarrow J/\psi p]$, $Br[P_c^+(4440) \rightarrow J/\psi p]$ and $Br[P_c^+(4457) \rightarrow J/\psi p]$, which are expected from preliminary results of the JLab E12-16-007 experiment [17]. According to them, upper limits on the cross sections (52) for $P_c^+(4312)$, $P_c^+(4440)$ and $P_c^+(4457)$ states almost an order of magnitude below the respective GlueX limits [4]. With this and within the representation of Eq. (52), we readily obtain the following relation between upper limits on the above branching fractions, which are expected from the J/ψ -007 experiment, and those already available from the GlueX experiment: $Br_{J/\psi-007}[P_{ci}^+ \rightarrow J/\psi p] \approx (1/\sqrt{10}) Br_{\text{GlueX}}[P_{ci}^+ \rightarrow J/\psi p]$ ($i = 1, 3, 4$). Model-dependent upper limits on the latter ratios of 4.6%, 2.3% and 3.8% for $P_c^+(4312)$, $P_c^+(4440)$ and $P_c^+(4457)$, assuming for each P_{ci}^+ spin-parity combination $J^P = (3/2)^-$, were set by the GlueX Collaboration [4]. So that, following the above relation, we get that $Br_{J/\psi-007}[P_c^+(4312) \rightarrow J/\psi p] \approx 1.46\%$, $Br_{J/\psi-007}[P_c^+(4440) \rightarrow J/\psi p] \approx 0.73\%$ and $Br_{J/\psi-007}[P_c^+(4457) \rightarrow J/\psi p] \approx 1.20\%$. This means that our choice of 1% for upper value of the branching ratios $Br[P_{ci}^+ \rightarrow J/\psi p]$ for all 4 states is quite reasonable and justified.

Accounting for the fact that the most of the narrow P_{ci}^+ and P_{ci}^0 resonances ($i = 1, 2, 3, 4$), having vacuum total decay widths in their rest frames of 9.8, 29.0, 20.6 and 6.4 MeV [2, 3], respectively, decay to $J/\psi p$ and $J/\psi n$ outside of the considered target nuclei [6] as well as the results presented both in Refs. [6, 7, 10] and above by Eqs. (3), (4), (51), (52), we can obtain the following expression for the J/ψ inclusive differential cross section arising from the production and decay of intermediate resonances P_{ci}^+ and P_{ci}^0 in γA reactions:

$$\begin{aligned} \frac{d\sigma_{\gamma A \rightarrow J/\psi X}^{(\text{sec})}(\mathbf{p}_\gamma, \mathbf{p}_{J/\psi})}{d\mathbf{p}_{J/\psi}} &= \frac{d\sigma_{\gamma A \rightarrow P_{ci}^+ \rightarrow J/\psi p}^{(\text{sec})}(\mathbf{p}_\gamma, \mathbf{p}_{J/\psi})}{d\mathbf{p}_{J/\psi}} + \frac{d\sigma_{\gamma A \rightarrow P_{ci}^0 \rightarrow J/\psi n}^{(\text{sec})}(\mathbf{p}_\gamma, \mathbf{p}_{J/\psi})}{d\mathbf{p}_{J/\psi}} = \\ &= I_V[A, \sigma_{P_c N}^{\text{in}}] \left\langle \frac{d\sigma_{\gamma p \rightarrow P_{ci}^+ \rightarrow J/\psi p}(\mathbf{p}_\gamma, \mathbf{p}_{J/\psi})}{d\mathbf{p}_{J/\psi}} \right\rangle_A, \quad i = 1, 2, 3, 4, \end{aligned} \quad (53)$$

where

$$\left\langle \frac{d\sigma_{\gamma p \rightarrow P_{ci}^+ \rightarrow J/\psi p}(\mathbf{p}_\gamma, \mathbf{p}_{J/\psi})}{d\mathbf{p}_{J/\psi}} \right\rangle_A = \int \int P_A(\mathbf{p}_t, E) d\mathbf{p}_t dE \left[\frac{d\sigma_{\gamma p \rightarrow P_{ci}^+ \rightarrow J/\psi p}(\sqrt{s^*}, \mathbf{p}_{J/\psi})}{d\mathbf{p}_{J/\psi}} \right], \quad (54)$$

and

$$\frac{d\sigma_{\gamma p \rightarrow P_{ci}^+ \rightarrow J/\psi p}(\sqrt{s^*}, \mathbf{p}_{J/\psi})}{d\mathbf{p}_{J/\psi}} = \sigma_{\gamma p \rightarrow P_{ci}^+}(\sqrt{s^*}, \Gamma_{ci}^+) \theta[\sqrt{s^*} - (m_{J/\psi} + m_p)] \times \quad (55)$$

$$\times \frac{1}{\Gamma_{ci}^+(\sqrt{s^*}, \mathbf{p}_\gamma)} \int d\mathbf{p}_p \frac{d\Gamma_{P_{ci}^+ \rightarrow J/\psi p}(\sqrt{s^*}, \mathbf{p}_{J/\psi}, \mathbf{p}_p)}{d\mathbf{p}_{J/\psi} d\mathbf{p}_p},$$

$$\frac{d\Gamma_{P_{ci}^+ \rightarrow J/\psi p}(\sqrt{s^*}, \mathbf{p}_{J/\psi}, \mathbf{p}_p)}{d\mathbf{p}_{J/\psi} d\mathbf{p}_p} = \frac{1}{2E_{ci}^+} \frac{1}{2J+1} |M_{P_{ci}^+ \rightarrow J/\psi p}|^2 (2\pi)^4 \delta(E_{ci}^+ - E_{J/\psi} - E_p) \times \quad (56)$$

$$\times \delta(\mathbf{p}_{ci}^+ - \mathbf{p}_{J/\psi} - \mathbf{p}_p) \frac{1}{(2\pi)^3 2E_{J/\psi}} \frac{1}{(2\pi)^3 2E_p},$$

$$\Gamma_{ci}^+(\sqrt{s^*}, \mathbf{p}_\gamma) = \Gamma_{ci}^+ / \gamma_{ci}^+, \quad (57)$$

$$E_{ci}^+ = E_\gamma + E_t, \quad \mathbf{p}_{ci}^+ = \mathbf{p}_\gamma + \mathbf{p}_t, \quad \gamma_{ci}^+ = E_{ci}^+ / \sqrt{s^*}. \quad (58)$$

Here, E_p is the final proton total energy ($E_p = \sqrt{m_p^2 + \mathbf{p}_p^2}$) and $|M_{P_{ci}^+ \rightarrow J/\psi p}|^2$ is summarized over spin states of initial and final particles matrix element squared describing the decays (43) for given i . The quantity $I_V[A, \sigma_{P_c N}^{\text{in}}]$ in Eq. (53) is defined above by Eq. (4), in which one needs to make the substitution $\sigma \rightarrow \sigma_{P_c N}^{\text{in}}$. Here the quantity $\sigma_{P_c N}^{\text{in}}$ denotes the inelastic total cross sections of the free $P_c N$ interaction. Our estimates [6]¹¹⁾, based on the $J/\psi p$ molecular scenario for the P_c^+ pentaquarks, show that this quantity can be evaluated as $\sigma_{P_c N}^{\text{in}} \approx 33.5$ mb. We will use this value throughout our calculations. In view of the aforesaid, the hidden-charm pentaquarks P_{ci}^+ (and P_{ci}^0) decays to $J/\psi p$ (and $J/\psi n$) are dominated by the lowest partial s -waves with zero relative orbital angular momentum. This implies that the matrix elements squared $|M_{P_{ci}^+ \rightarrow J/\psi p}|^2$ (and $|M_{P_{ci}^0 \rightarrow J/\psi n}|^2$) lead to an isotropic angular distributions of the $P_{ci}^+ \rightarrow J/\psi p$ (and $P_{ci}^0 \rightarrow J/\psi n$) decays for the considered spin-parity assignments of the P_{ci}^+ (and P_{ci}^0) states. With this, we can readily obtain the following relation between $|M_{P_{ci}^+ \rightarrow J/\psi p}|^2$ and the partial width $\Gamma_{P_{ci}^+ \rightarrow J/\psi p}$ of the $P_{ci}^+ \rightarrow J/\psi p$ decay (cf. [10]):

$$\frac{1}{2J+1} \frac{|M_{P_{ci}^+ \rightarrow J/\psi p}|^2}{(2\pi)^2} = \frac{2s^*}{\pi p_{J/\psi}^*} \Gamma_{P_{ci}^+ \rightarrow J/\psi p}. \quad (59)$$

With it, we find for the expression (55) a more simpler form (cf. Eq. (9)):

$$\frac{d\sigma_{\gamma p \rightarrow P_{ci}^+ \rightarrow J/\psi p}(\sqrt{s^*}, \mathbf{p}_{J/\psi})}{d\mathbf{p}_{J/\psi}} = \sigma_{\gamma p \rightarrow P_{ci}^+}(\sqrt{s^*}, \Gamma_{ci}^+) \theta[\sqrt{s^*} - (m_{J/\psi} + m_p)] \times \quad (60)$$

$$\times \frac{1}{I_2(s^*, m_{J/\psi}, m_p)} Br[P_{ci}^+ \rightarrow J/\psi p] \frac{1}{4E_{J/\psi}} \frac{1}{(\omega + E_t)} \delta[\omega + E_t - \sqrt{m_p^2 + (\mathbf{Q} + \mathbf{p}_t)^2}],$$

where the quantities ω and \mathbf{Q} are defined above by Eq. (12). We will employ this expression in our calculations of the J/ψ momentum distribution from the processes (41)–(44) in γA reactions. Integrating the differential cross section (53) over the angular range of $\Delta\Omega_{J/\psi=0^\circ} \leq \theta_{J/\psi} \leq 20^\circ$, $0 \leq \varphi_{J/\psi} \leq 2\pi$ of our interest, we represent this distribution for given i in this angular range in the following form (cf. Eq. (24)):

$$\frac{d\sigma_{\gamma A \rightarrow J/\psi X}^{(\text{sec})}(p_\gamma, p_{J/\psi})}{dp_{J/\psi}} = \int_{\Delta\Omega_{J/\psi}} d\Omega_{J/\psi} \frac{d\sigma_{\gamma A \rightarrow J/\psi X}^{(\text{sec})}(\mathbf{p}_\gamma, \mathbf{p}_{J/\psi})}{d\mathbf{p}_{J/\psi}} p_{J/\psi}^2 \quad (61)$$

¹¹⁾These estimates also show that we can neglect quasielastic $P_{ci}^+ N$ and $P_{ci}^0 N$ rescatterings in their way out of the target nucleus.

$$= 2\pi I_V[A, \sigma_{P_{cN}}^{\text{in}}] \int_{\cos 20^\circ}^1 d\cos\theta_{J/\psi} \left\langle \frac{d\sigma_{\gamma p \rightarrow P_{ci}^+ \rightarrow J/\psi p}(p_\gamma, p_{J/\psi}, \theta_{J/\psi})}{dp_{J/\psi} d\Omega_{J/\psi}} \right\rangle_A, \quad i = 1, 2, 3, 4.$$

Before going to the next step, we calculate the free space resonant J/ψ energy distribution $d\sigma_{\gamma p \rightarrow P_{ci}^+ \rightarrow J/\psi p}[\sqrt{s}, p_{J/\psi}]/dE_{J/\psi}$ from the two-step processes (41)/(43), proceeding on the free target proton at rest, in addition to that from the background $\gamma p \rightarrow J/\psi p$ reaction (cf. Eq. (39)). The energy-momentum conservation in these processes leads to the conclusion that the kinematical characteristics of J/ψ mesons produced in them and in this reaction are the same at given incident photon energy. The full on-shell differential cross section $d\sigma_{\gamma p \rightarrow P_{ci}^+ \rightarrow J/\psi p}[\sqrt{s}, \mathbf{p}_{J/\psi}]/d\mathbf{p}_{J/\psi}$ can be obtained from more general one (60) in the limits: $\mathbf{p}_t \rightarrow 0$, $E_t \rightarrow m_p$ and $s^* \rightarrow s$. Its integration over the laboratory polar angle $\theta_{J/\psi}$, when this angle belongs to the allowed angular interval (25), gives:

$$\begin{aligned} \frac{d\sigma_{\gamma p \rightarrow P_{ci}^+ \rightarrow J/\psi p}[\sqrt{s}, p_{J/\psi}]}{dE_{J/\psi}} &= 2\pi \int_{\cos\theta_{J/\psi}^{\text{max}}}^1 d\cos\theta_{J/\psi} p_{J/\psi} E_{J/\psi} \frac{d\sigma_{\gamma p \rightarrow P_{ci}^+ \rightarrow J/\psi p}[\sqrt{s}, \mathbf{p}_{J/\psi}]}{d\mathbf{p}_{J/\psi}} = \\ &= \sigma_{\gamma p \rightarrow P_{ci}^+}(\sqrt{s}, \Gamma_{ci}^+) \theta[\sqrt{s} - (m_{J/\psi} + m_p)] \times \\ &\times \left(\frac{\sqrt{s}}{2p_\gamma p_{J/\psi}^*} \right) Br[P_{ci}^+ \rightarrow J/\psi p] \text{ for } E_{J/\psi}^{(2)}(0^\circ) \leq E_{J/\psi} \leq E_{J/\psi}^{(1)}(0^\circ). \end{aligned} \quad (62)$$

Eq. (62) shows that the free space J/ψ energy distribution, which arises from the production/decay chains (41)/(43), exhibits a completely flat behavior within the allowed energy range (38).

3. Results

The free space direct non-resonant J/ψ production total cross section (23) (solid curve), the total cross section for the resonant J/ψ production in the processes (41)/(43) determined on the basis of Eq. (52) for the considered spin-parity assignments of the hidden-charm resonances P_{ci}^+ ($i = 1, 2, 3, 4$) and for branching ratios $Br[P_{ci}^+ \rightarrow J/\psi p] = 1\%$ for all four P_{ci}^+ states (short-dashed curve) and the combined (non-resonant plus resonant) J/ψ production total cross section (dotted curve) are presented in Fig. 4 as functions of photon energy. It can be seen from this figure that the $P_c^+(4312)$ and $P_c^+(4337)$ as well as $P_c^+(4440)$ and $P_c^+(4457)$ resonances exhibit itself as two narrow overlapping peaks, respectively, at $E_\gamma = 9.44$ and $E_\gamma = 9.554$ GeV as well as at $E_\gamma = 10.04$ and $E_\gamma = 10.12$ GeV. The strengths of these four peaks reach a value $\sim 0.1\text{--}0.2$ nb. Whereas, the non-resonant contribution in the resonance region is of about 1 nb. As a result, the combined total cross section of the reaction $\gamma p \rightarrow J/\psi p$ has no distinct peak structures, corresponding to the P_{ci}^+ states, and it is practically not distinguished from that for the background reaction. If $Br[P_{ci}^+ \rightarrow J/\psi p] = 0.25$ and 0.5% , then the resonant J/ψ yield will be even more less than the non-resonant one. This means that will be very hard to measure the P_{ci}^+ pentaquark states in J/ψ total photoproduction cross section on a proton target in the near-threshold energy region. Evidently, to see their experimentally one needs to consider such observable, which is appreciably sensitive to the P_c^+ signal in some region of the available phase space. For example, the large t region of the differential cross section $d\sigma/dt$ in the J/ψ -007 experiment [17], where the t -dependence of the background J/ψ meson production is suppressed while its resonant production is rather flat. This is also supported by the findings of Ref. [25], where the photoproduction of initially claimed by the LHCb Collaboration hidden charm pentaquark states $P_c^+(4380)$ and $P_c^+(4450)$ with the spin-parity assignments of $(3/2^-, 5/2^+)$ or $(3/2^+, 5/2^-)$, respectively, on the proton target was considered by including the t -channel diffractive Pomeron exchanges and the s -channel pentaquark productions.

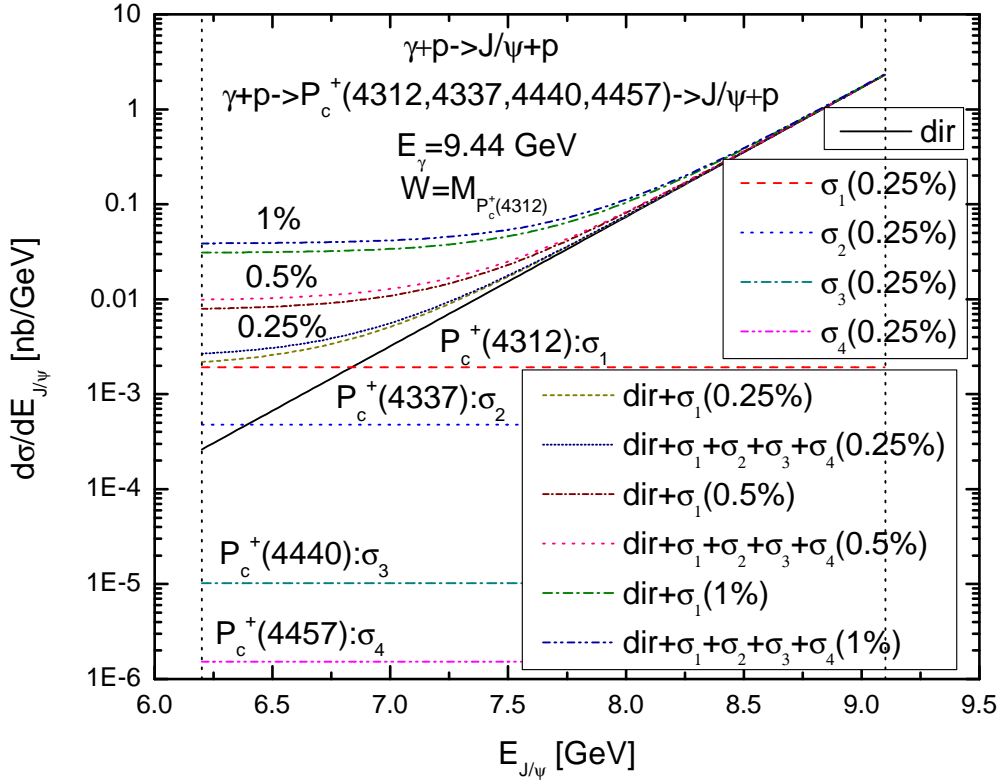


Figure 5: (Color online) The direct non-resonant J/ψ energy distribution in the free space elementary process $\gamma p \rightarrow J/\psi p$, calculated in line with Eq. (39) at initial photon resonant energy of 9.44 GeV in the laboratory system (solid curve). The resonant J/ψ energy distributions in the two-step processes $\gamma p \rightarrow P_c^+(4312) \rightarrow J/\psi p$, $\gamma p \rightarrow P_c^+(4337) \rightarrow J/\psi p$, $\gamma p \rightarrow P_c^+(4440) \rightarrow J/\psi p$ and $\gamma p \rightarrow P_c^+(4457) \rightarrow J/\psi p$, calculated in line with Eq. (62) at the same incident photon energy of 9.44 GeV assuming that the resonances $P_c^+(4312)$, $P_c^+(4337)$, $P_c^+(4440)$ and $P_c^+(4457)$ with the spin-parity assignments $J^P = (1/2)^-$, $J^P = (1/2)^-$, $J^P = (1/2)^-$ and $J^P = (3/2)^-$, correspondingly, all decay to the $J/\psi p$ with branching fractions 0.25% (respectively, red dashed, blue dotted, dark cyan dashed-dotted and magenta dashed-dotted-dotted curves). Incoherent sum of the direct non-resonant J/ψ energy distribution and resonant ones, calculated supposing that the resonances $P_c^+(4312)$ and $P_c^+(4312)$, $P_c^+(4337)$, $P_c^+(4440)$, $P_c^+(4457)$ with the same spin-parity combinations all decay to the $J/\psi p$ with branching fractions 0.25, 0.5 and 1% (respectively, dark yellow short-dashed, wine short-dashed-dotted, olive dashed-dotted and navy short-dotted, pink dotted, royal dashed-dotted-dotted curves), all as functions of the total J/ψ energy $E_{J/\psi}$ in the laboratory system. The vertical dotted lines indicate the range of J/ψ allowed energies in this system for the considered direct non-resonant and resonant J/ψ production off a free target proton at rest at given initial photon resonant energy of 9.44 GeV.

Here, by assuming that the pentaquark states decay into the $J/\psi p$ mode with fraction of 5% was, in particular, shown that the contributions from the P_c^+ states calculated at resonant c.m. energies $W = 4.38$ GeV and 4.45 GeV for the two spin-parity combinations considered make the differential cross section of the $\gamma p \rightarrow J/\psi p$ reaction strongly deviated from the diffractive one at off-forward angles in the c.m. frame. This cross section indeed is rather flat at these angles and overestimates at them significantly the contributions from the diffractive Pomeron exchanges. Furthermore, the

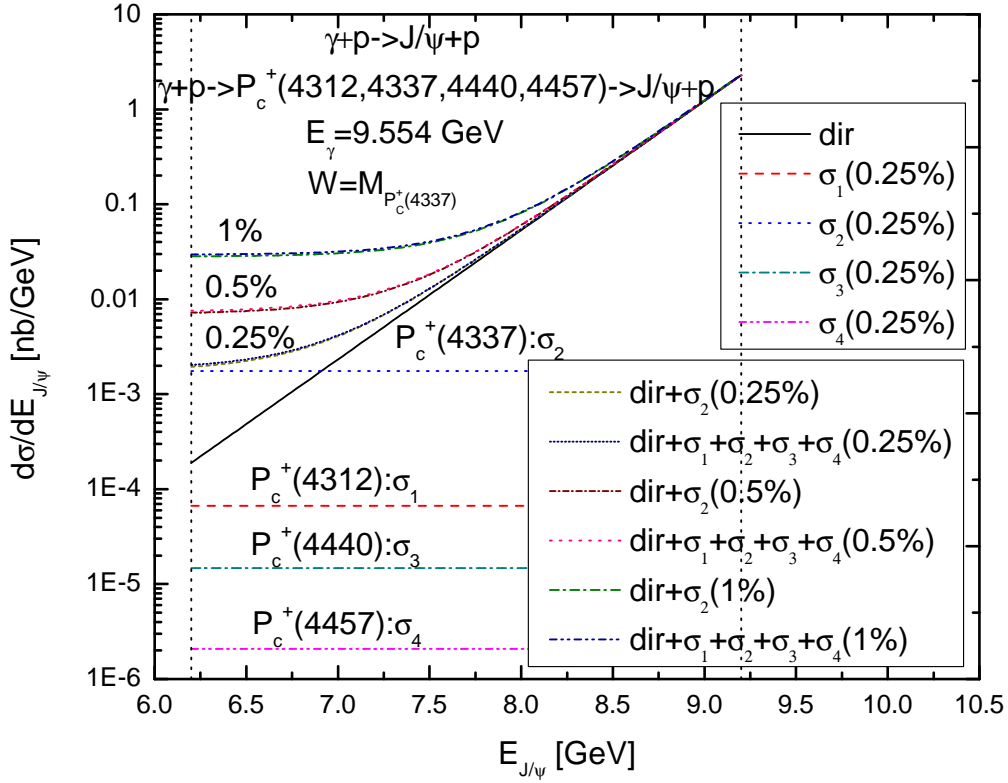


Figure 6: (Color online) The direct non-resonant J/ψ energy distribution in the free space elementary process $\gamma p \rightarrow J/\psi p$, calculated in line with Eq. (39) at initial photon resonant energy of 9.554 GeV in the laboratory system (solid curve). The resonant J/ψ energy distributions in the two-step processes $\gamma p \rightarrow P_c^+(4312) \rightarrow J/\psi p$, $\gamma p \rightarrow P_c^+(4337) \rightarrow J/\psi p$, $\gamma p \rightarrow P_c^+(4440) \rightarrow J/\psi p$ and $\gamma p \rightarrow P_c^+(4457) \rightarrow J/\psi p$, calculated in line with Eq. (62) at the same incident photon energy of 9.554 GeV assuming that the resonances $P_c^+(4312)$, $P_c^+(4337)$, $P_c^+(4440)$ and $P_c^+(4457)$ with the spin-parity assignments $J^P = (1/2)^-$, $J^P = (1/2)^-$, $J^P = (1/2)^-$ and $J^P = (3/2)^-$, correspondingly, all decay to the $J/\psi p$ with branching fractions 0.25% (respectively, red dashed, blue dotted, dark cyan dashed-dotted and magenta dashed-dotted-dotted curves). Incoherent sum of the direct non-resonant J/ψ energy distribution and resonant ones, calculated supposing that the resonances $P_c^+(4337)$ and $P_c^+(4312)$, $P_c^+(4337)$, $P_c^+(4440)$, $P_c^+(4457)$ with the same spin-parity combinations all decay to the $J/\psi p$ with branching fractions 0.25, 0.5 and 1% (respectively, dark yellow short-dashed, wine short-dashed-dotted, olive dashed-dotted and navy short-dotted, pink dotted, royal dashed-dotted-dotted curves), all as functions of the total J/ψ energy $E_{J/\psi}$ in the laboratory system. The vertical dotted lines indicate the range of J/ψ allowed energies in this system for the considered direct non-resonant and resonant J/ψ production off a free target proton at rest at given initial photon resonant energy of 9.554 GeV.

predictions for the differential cross section of the $\gamma p \rightarrow J/\psi p$ reaction, obtained in Ref. [26] within the approach in which the Pomeron-exchange model with the parameters determined from fitting the available total cross section data up to $W = 300$ GeV is used to calculate the non-resonant amplitudes as well as the partial decay widths of nucleon resonances with hidden charm, $N_{c\bar{c}}^*$, predicted by the considered meson-baryons (MB) coupled-channel models to estimate the $N_{c\bar{c}}^* \rightarrow MB$ transition matrix elements and the vector-meson dominance model to evaluate $\gamma p \rightarrow N_{c\bar{c}}^*$

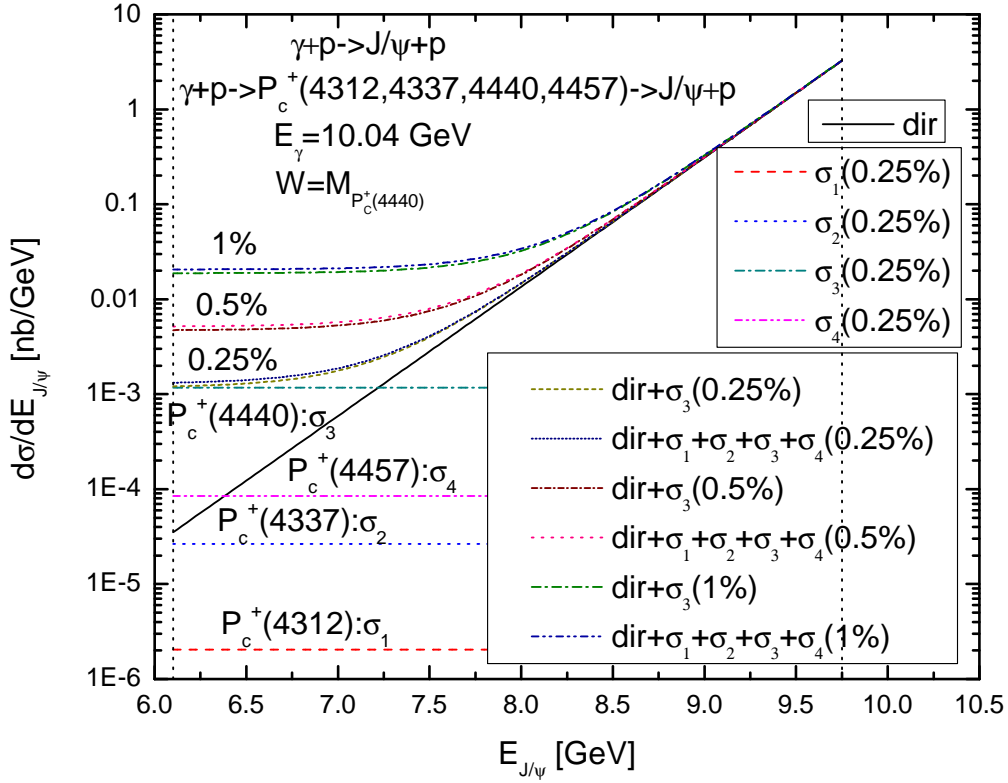


Figure 7: (Color online) The direct non-resonant J/ψ energy distribution in the free space elementary process $\gamma p \rightarrow J/\psi p$, calculated in line with Eq. (39) at initial photon resonant energy of 10.04 GeV in the laboratory system (solid curve). The resonant J/ψ energy distributions in the two-step processes $\gamma p \rightarrow P_c^+(4312) \rightarrow J/\psi p$, $\gamma p \rightarrow P_c^+(4337) \rightarrow J/\psi p$, $\gamma p \rightarrow P_c^+(4440) \rightarrow J/\psi p$ and $\gamma p \rightarrow P_c^+(4457) \rightarrow J/\psi p$, calculated in line with Eq. (62) at the same incident photon energy of 10.04 GeV assuming that the resonances $P_c^+(4312)$, $P_c^+(4337)$, $P_c^+(4440)$ and $P_c^+(4457)$ with the spin-parity assignments $J^P = (1/2)^-$, $J^P = (1/2)^-$, $J^P = (1/2)^-$ and $J^P = (3/2)^-$, correspondingly, all decay to the $J/\psi p$ with branching fractions 0.25% (respectively, red dashed, blue dotted, dark cyan dashed-dotted and magenta dashed-dotted-dotted curves). Incoherent sum of the direct non-resonant J/ψ energy distribution and resonant ones, calculated supposing that the resonances $P_c^+(4440)$ and $P_c^+(4312)$, $P_c^+(4337)$, $P_c^+(4440)$, $P_c^+(4457)$ with the same spin-parity combinations all decay to the $J/\psi p$ with branching fractions 0.25, 0.5 and 1% (respectively, dark yellow short-dashed, wine short-dashed-dotted, olive dashed-dotted and navy short-dotted, pink dotted, royal dashed-dotted-dotted curves), all as functions of the total J/ψ energy $E_{J/\psi}$ in the laboratory system. The vertical dotted lines indicate the range of J/ψ allowed energies in this system for the considered direct non-resonant and resonant J/ψ production off a free target proton at rest at given initial photon resonant energy of 10.04 GeV.

as $\gamma p \rightarrow V p \rightarrow N_{cc}^*$ with $V = \rho, \omega, J/\psi$ are adopted, demonstrate that the N_{cc}^* can be readily identified in the near-threshold differential cross section of the $\gamma p \rightarrow J/\psi p$ process at large angles where the contribution from Pomeron exchanges becomes insignificant. It should also be noted that an earlier prediction of the differential cross section of this process, made in Ref. [27] at the resonant energy point $W = 4.412$ GeV by considering the non-resonant ($\gamma p \rightarrow J/\psi p$) and resonant ($\gamma p \rightarrow N_{cc}^*(4412) \rightarrow J/\psi p$) $J/\psi p$ photoproduction using, respectively, the two gluon and

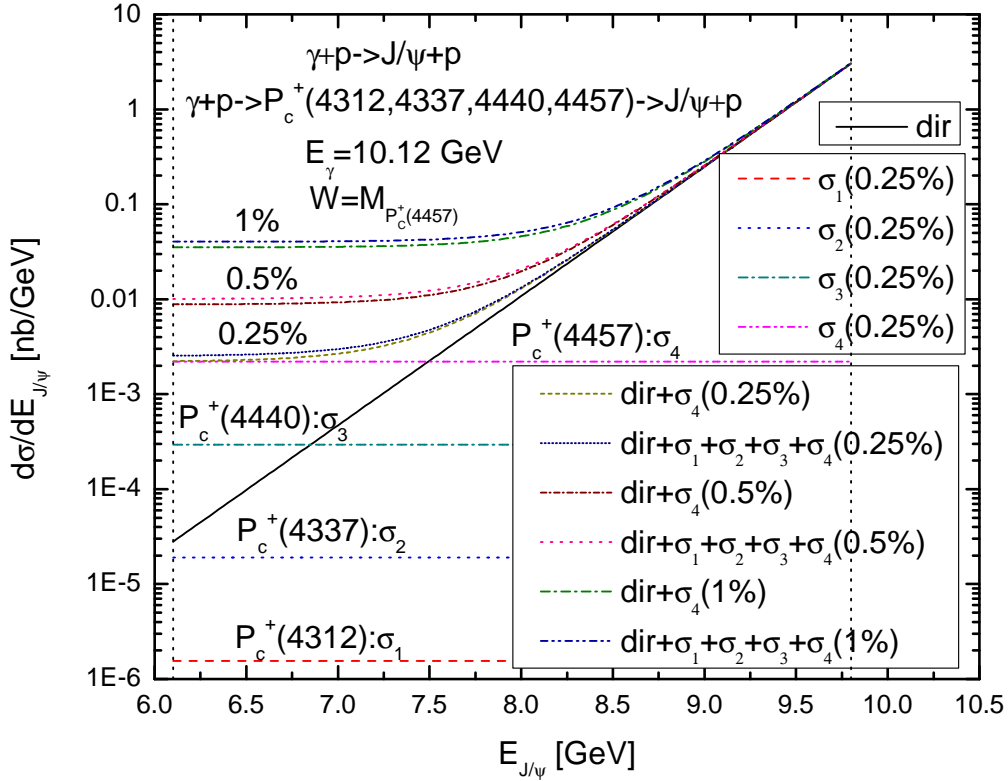


Figure 8: (Color online) The direct non-resonant J/ψ energy distribution in the free space elementary process $\gamma p \rightarrow J/\psi p$, calculated in line with Eq. (39) at initial photon resonant energy of 10.12 GeV in the laboratory system (solid curve). The resonant J/ψ energy distributions in the two-step processes $\gamma p \rightarrow P_c^+(4312) \rightarrow J/\psi p$, $\gamma p \rightarrow P_c^+(4337) \rightarrow J/\psi p$, $\gamma p \rightarrow P_c^+(4440) \rightarrow J/\psi p$ and $\gamma p \rightarrow P_c^+(4457) \rightarrow J/\psi p$, calculated in line with Eq. (62) at the same incident photon energy of 10.12 GeV assuming that the resonances $P_c^+(4312)$, $P_c^+(4337)$, $P_c^+(4440)$ and $P_c^+(4457)$ with the spin-parity assignments $J^P = (1/2)^-$, $J^P = (1/2)^-$, $J^P = (1/2)^-$ and $J^P = (3/2)^-$, correspondingly, all decay to the $J/\psi p$ with branching fractions 0.25% (respectively, red dashed, blue dotted, dark cyan dashed-dotted and magenta dashed-dotted-dotted curves). Incoherent sum of the direct non-resonant J/ψ energy distribution and resonant ones, calculated supposing that the resonances $P_c^+(4457)$ and $P_c^+(4312)$, $P_c^+(4337)$, $P_c^+(4440)$, $P_c^+(4457)$ with the same spin-parity combinations all decay to the $J/\psi p$ with branching fractions 0.25, 0.5 and 1% (respectively, dark yellow short-dashed, wine short-dashed-dotted, olive dashed-dotted and navy short-dotted, pink dotted, royal dashed-dotted-dotted curves), all as functions of the total J/ψ energy $E_{J/\psi}$ in the laboratory system. The vertical dotted lines indicate the range of J/ψ allowed energies in this system for the considered direct non-resonant and resonant J/ψ production off a free target proton at rest at given initial photon resonant energy of 10.12 GeV.

three gluon exchange model [14] and vector-meson dominance model to generate vector mesons $\rho, \omega, J/\psi$ from photon which rescatter with the target proton to form intermediate hidden charmed nucleon resonance $N_{cc}^*(4412)$, shows as well that this cross section is quite weakly dependent on the c.m.s. J/ψ production angle. It should be additionally pointed out that the feasibility of detecting the $P_c^+(4450)$ resonance with the spin-parity quantum numbers $J^P = 3/2^-$ and $J^P = 5/2^+$ in near-threshold J/ψ photoproduction off protons in the CLAS12 experiment at JLab was

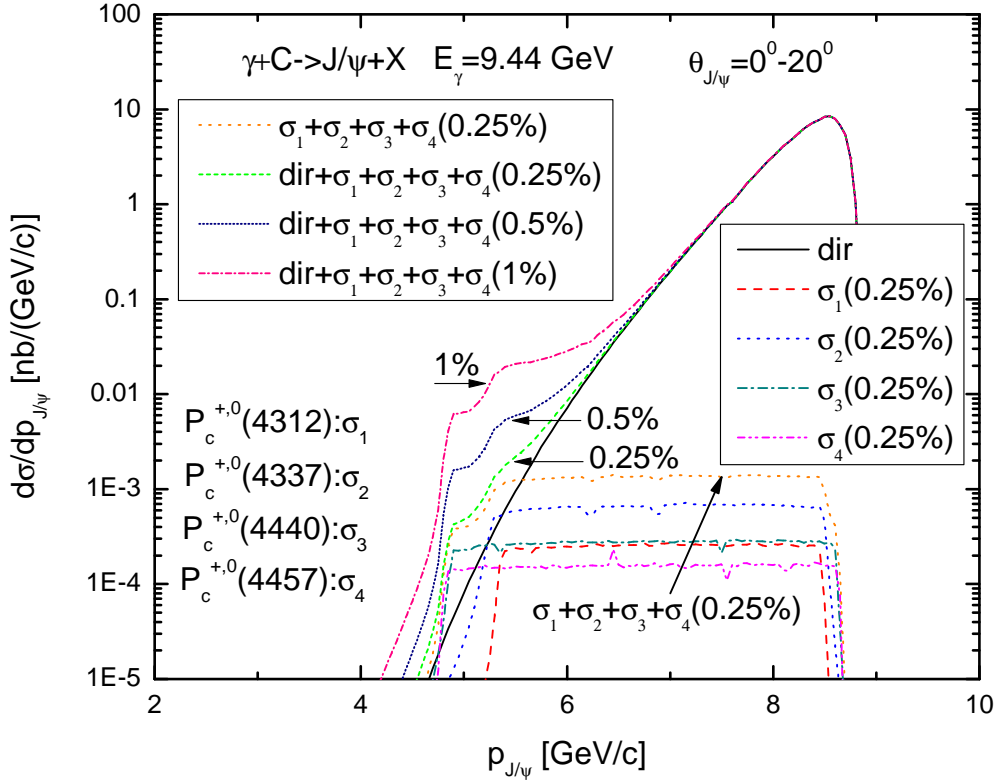


Figure 9: (Color online) The direct non-resonant momentum distribution of J/ψ mesons, produced in the reaction $\gamma^{12}\text{C} \rightarrow J/\psi X$ in the laboratory polar angular range of 0° – 20° and calculated in line with Eq. (24) at initial photon resonant energy of 9.44 GeV in the laboratory system (solid curve). The resonant momentum distributions of J/ψ mesons, produced in the two-step processes $\gamma p(n) \rightarrow P_c^+(4312)(P_c^0(4312)) \rightarrow J/\psi p(n)$, $\gamma p(n) \rightarrow P_c^+(4337)(P_c^0(4337)) \rightarrow J/\psi p(n)$, $\gamma p(n) \rightarrow P_c^+(4440)(P_c^0(4440)) \rightarrow J/\psi p(n)$ and $\gamma p(n) \rightarrow P_c^+(4457)(P_c^0(4457)) \rightarrow J/\psi p(n)$ and calculated in line with Eq. (61) at the same incident photon energy of 9.44 GeV assuming that the resonances $P_c^{+,0}(4312)$, $P_c^{+,0}(4337)$, $P_c^{+,0}(4440)$ and $P_c^{+,0}(4457)$ with the spin-parity assignments $J^P = (1/2)^-$, $J^P = (1/2)^-$, $J^P = (1/2)^-$ and $J^P = (3/2)^-$, correspondingly, all decay to the $J/\psi p(n)$ with branching fractions 0.25% (respectively, red dashed, blue dotted, dark cyan dashed-dotted and magenta dashed-dotted-dotted curves) and their incoherent sum (orange dotted curve). Incoherent sum of the direct non-resonant J/ψ momentum distribution and resonant ones, calculated supposing that the resonances $P_c^{+,0}(4312)$, $P_c^{+,0}(4337)$, $P_c^{+,0}(4440)$, $P_c^{+,0}(4457)$ with the same spin-parity combinations all decay to the $J/\psi p(n)$ with branching fractions 0.25, 0.5 and 1% (respectively, green short-dashed, navy short-dotted and pink short-dashed-dotted curves), all as functions of the J/ψ momentum $p_{J/\psi}$ in the laboratory frame.

also discussed in Ref. [23] in the framework of a two-component model containing the directly produced resonance, diffractive background and accounting for the experimental resolution effects. The contribution of the $P_c^+(4450)$ state, produced through the vector-meson dominance mechanism, was parametrized using the Breit-Wigner ansatz and the non-resonant contribution was described by the Pomeron exchanges. The fit of the available at that time data points for differential cross section of the $\gamma p \rightarrow J/\psi p$ reaction, with $|t| \leq 1.5 \text{ GeV}^2$, covering energy range from threshold to $E_\gamma \sim 120 \text{ TeV}$ in the lab frame, with this model showed that the upper limits for branching ratio

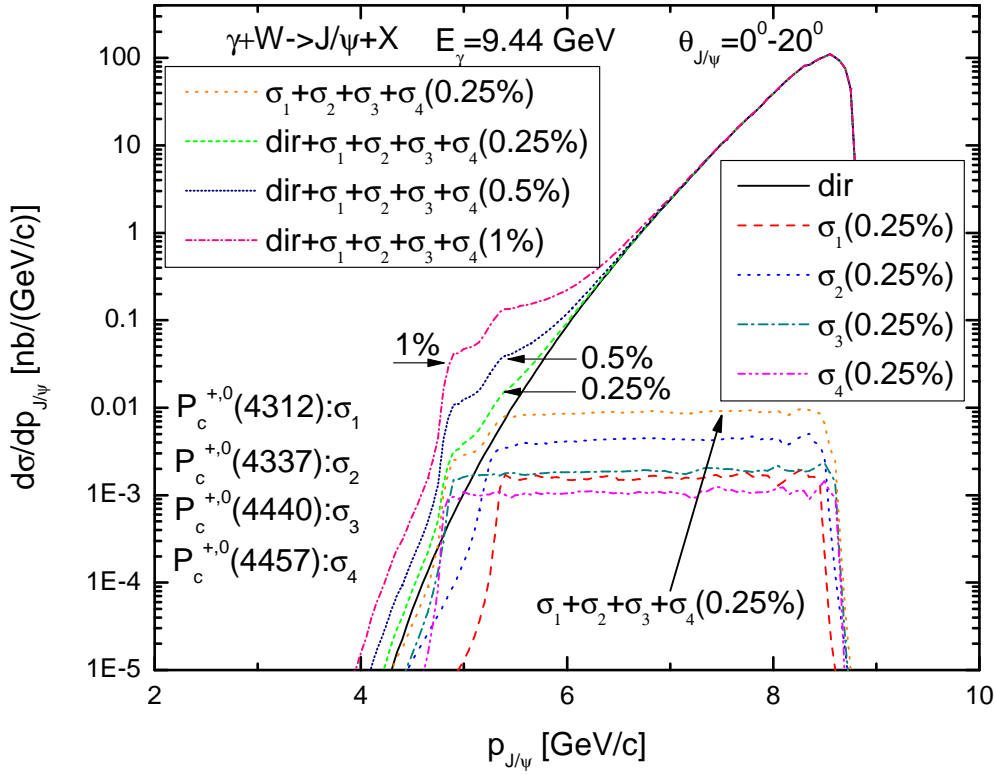


Figure 10: (Color online) The direct non-resonant momentum distribution of J/ψ mesons, produced in the reaction $\gamma^{184}\text{W} \rightarrow J/\psi X$ in the laboratory polar angular range of 0° – 20° and calculated in line with Eq. (24) at initial photon resonant energy of 9.44 GeV in the laboratory system (solid curve). The resonant momentum distributions of J/ψ mesons, produced in the two-step processes $\gamma p(n) \rightarrow P_c^+(4312)(P_c^0(4312)) \rightarrow J/\psi p(n)$, $\gamma p(n) \rightarrow P_c^+(4337)(P_c^0(4337)) \rightarrow J/\psi p(n)$, $\gamma p(n) \rightarrow P_c^+(4440)(P_c^0(4440)) \rightarrow J/\psi p(n)$ and $\gamma p(n) \rightarrow P_c^+(4457)(P_c^0(4457)) \rightarrow J/\psi p(n)$ and calculated in line with Eq. (61) at the same incident photon energy of 9.44 GeV assuming that the resonances $P_c^{+,0}(4312)$, $P_c^{+,0}(4337)$, $P_c^{+,0}(4440)$ and $P_c^{+,0}(4457)$ with the spin-parity assignments $J^P = (1/2)^-$, $J^P = (1/2)^-$, $J^P = (1/2)^-$ and $J^P = (3/2)^-$, correspondingly, all decay to the $J/\psi p(n)$ with branching fractions 0.25% (respectively, red dashed, blue dotted, dark cyan dashed-dotted and magenta dashed-dotted-dotted curves) and their incoherent sum (orange dotted curve). Incoherent sum of the direct non-resonant J/ψ momentum distribution and resonant ones, calculated supposing that the resonances $P_c^{+,0}(4312)$, $P_c^{+,0}(4337)$, $P_c^{+,0}(4440)$, $P_c^{+,0}(4457)$ with the same spin-parity combinations all decay to the $J/\psi p(n)$ with branching fractions 0.25, 0.5 and 1% (respectively, green short-dashed, navy short-dotted and pink short-dashed-dotted curves), all as functions of the J/ψ momentum $p_{J/\psi}$ in the laboratory frame.

$Br[P_c^+(4450) \rightarrow J/\psi p]$ of the $P_c^+(4450)$ pentaquark range from 23% to 30% for $J = 3/2$, depending on the experimental resolution, and from 8% to 17% for $J = 5/2$. These are essentially larger than those of several percent set later on by the GlueX Collaboration [4]. Finally, it is worth noting that the photoproduction of the J/ψ off the proton near threshold was studied in Ref. [28] using a novel final $J/\psi p$ production mechanism via the open charm $\Lambda_c^+ \bar{D}^0$ and $\Lambda_c^+ \bar{D}^{*0}$ intermediate states. The authors found that the existing experimental data [4] on $\gamma p \rightarrow J/\psi p$ can be well described within the suggested mechanism. Moreover, they identified a clear experimental signature for this

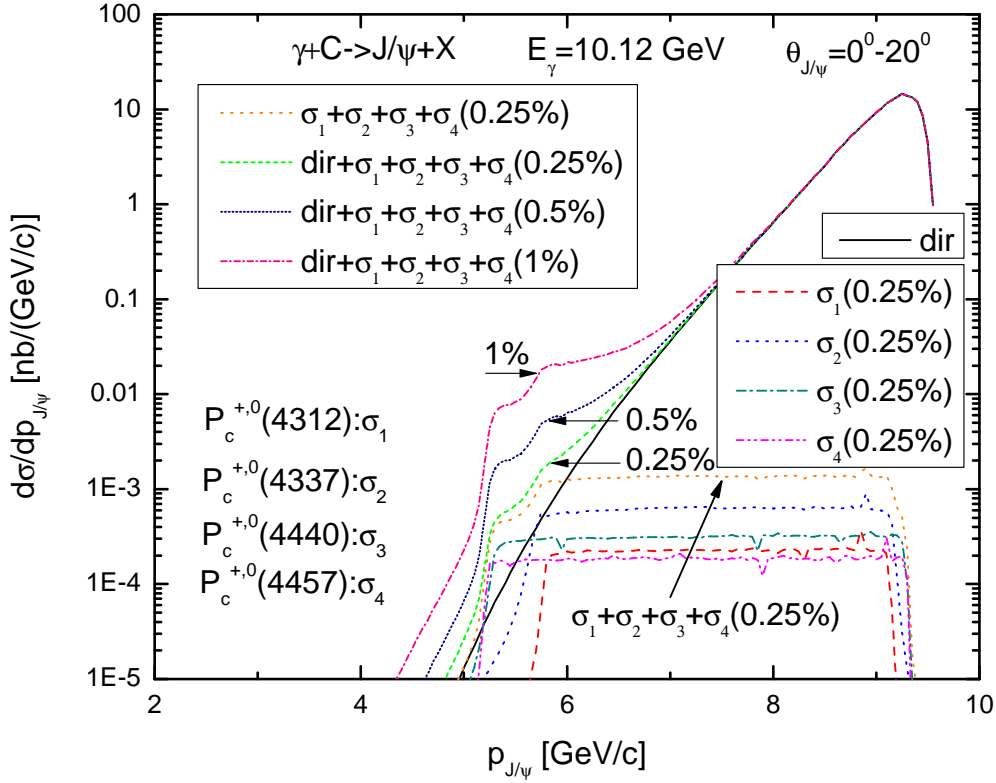


Figure 11: (Color online) The same as in Fig. 9, but for the initial photon energy of 10.12 GeV.

mechanism: within it must be pronounced cusps at the $\Lambda_c^+ \bar{D}^0$ and $\Lambda_c^+ \bar{D}^{*0}$ thresholds in the energy dependence of the total cross section of the $\gamma p \rightarrow J/\psi p$ reaction, and found that the data [4] consistent with this feature within their accuracy. One may hope that further measurements of the J/ψ photoproduction off the proton at JLab with higher statistics than GlueX will provide a deeper understanding of the J/ψ photoproduction mechanism.

Taking into account the aforementioned, now we consider the J/ψ energy distribution from the considered $\gamma p \rightarrow J/\psi p$ elementary reaction. The model developed by us allows to calculate the direct non-resonant J/ψ energy distribution from this reaction, the resonant ones from the production/decay chains (41)/(43), proceeding on the free target proton being at rest. They were calculated according to Eqs. (39), (62), respectively, for incident photon resonant energies of 9.44, 9.554, 10.04 and 10.12 GeV. The resonant J/ψ energy distributions were determined for the considered spin-parity assignments of the $P_c^+(4312)$, $P_c^+(4337)$, $P_c^+(4440)$, $P_c^+(4457)$ resonances for branching fractions $Br[P_{ci}^+ \rightarrow J/\psi p] = 0.25\%$ for all four states. These dependencies, together with the incoherent sum of the non-resonant J/ψ energy distribution and resonant ones, calculated assuming that all the resonances $P_c^+(4312)$ and P_{ci}^+ ($i = 1, 2, 3, 4$), $P_c^+(4337)$ and P_{ci}^+ ($i = 1, 2, 3, 4$), $P_c^+(4440)$ and P_{ci}^+ ($i = 1, 2, 3, 4$), $P_c^+(4457)$ and P_{ci}^+ ($i = 1, 2, 3, 4$) decay to the $J/\psi p$ mode with three adopted options for the branching ratios $Br[P_{ci}^+ \rightarrow J/\psi p]$, as functions of the J/ψ total energy $E_{J/\psi}$ are shown, respectively, in Figs. 5, 6, 7, 8. It is seen from these figures that the resonant J/ψ production cross sections show a flat behavior at all allowed energies $E_{J/\psi}$. Whereas the non-resonant cross section drops fastly as $E_{J/\psi}$ decreases. At incident photon resonant energies of 9.44, 9.554, 10.04 and 10.12 GeV of interest its strength is essentially larger than those of the resonant J/ψ production cross sections, calculated for the value of the branching ratios $Br[P_{ci}^+ \rightarrow J/\psi p] = 0.25\%$

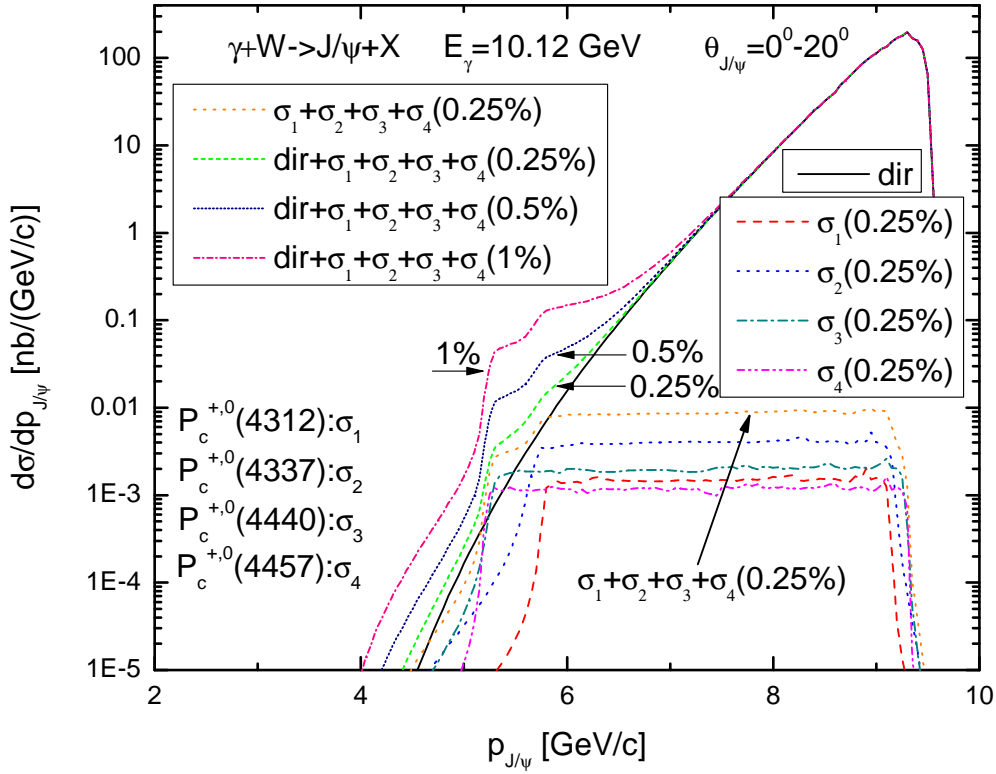


Figure 12: (Color online) The same as in Fig. 10, but for the initial photon energy of 10.12 GeV.

for "high" allowed J/ψ total energies greater than ≈ 7.25 GeV. Whereas at "low" J/ψ total energies (below 7.25 GeV) and for each considered photon energy the contribution from the resonance with the centroid at this energy, decaying to the $J/\psi p$ with the branching ratio of 0.25%, is much larger than the non-resonant one. Thus, for instance, in this case for the J/ψ mesons with total energy of 6.5 GeV their resonant production cross section is enhanced compared to the non-resonant one by sizeable factors of about 2.9, 3.6, 9.5 and 22.5 at initial photon energies of 9.44, 9.554, 10.04 and 10.12 GeV, respectively. Moreover, this contribution is also substantially larger than those, arising from the decays of another three pentaquarks to the $J/\psi p$ channel with the branching ratios $Br[P_{ci}^+ \rightarrow J/\psi p] = 0.25\%$, at the above-mentioned "low" J/ψ total energies. As a result, at each considered photon energy the J/ψ meson combined energy distribution, deriving from the direct J/ψ meson production and from the decay of the pentaquark resonance located at this energy to the $J/\psi p$ mode, reveals here a clear sensitivity to the adopted variations in the branching ratio of this decay. Thus, for example, for the J/ψ mesons with total energy of 6.5 GeV and for the lowest considered incident photon energy of 9.44 GeV this J/ψ combined distribution is enhanced for the values of this ratio of 0.25, 0.5 and 1% by notable factors of about 4.0, 12.5 and 46.8, respectively, as compared to that from the directly produced J/ψ mesons. And for the highest initial photon energy of 10.12 GeV of our interest, at which the resonance $P_c^+(4457)$ appears as peak structure in the total cross section of the exclusive reaction $\gamma p \rightarrow J/\psi p$, the analogous factors become much larger and they are of about 23.5, 90.8 and 360.3, respectively. Furthermore, one can see that the above "partial" combined energy distribution of the J/ψ mesons is practically indistinguishable from their "total" combined differential energy distribution, arising from the direct and resonant J/ψ meson production via the production/decay chains (41)/(43). This implies, on the one hand,

that the differences between the combined results, obtained by using a conservative value of the branching fractions of the decays $P_{ci}^+ \rightarrow J/\psi p$ of 0.25% and the non-resonant background, as well as between the combined results, determined by employing the values of the branching ratios of these decays of 0.25 and 0.5%, 0.5 and 1%, are quite sizeable and experimentally measurable at "low" charmonium total energies. On the other hand, at each incident photon resonant energy considered the observation here of the specific hidden-charm LHCb pentaquark will be practically not influenced by the presence of the another three hidden-charm pentaquark states and by the background reaction. Since the J/ψ production differential cross sections have a small absolute values ~ 0.01 – 0.1 nb/GeV at "low" J/ψ total energies $E_{J/\psi}$, their measurement requires both high luminosities and large-acceptance detectors. Such measurement might be performed in the near future at the JLab in Hall A within the planned here high-statistics (~ 800 k J/ψ events in photoproduction) and high-precision E12-12-006 experiment using the SoLID detector [5, 17].

The momentum dependencies of the absolute non-resonant, resonant and combined J/ψ meson differential cross sections, correspondingly, from the direct (1), (2), two-step (41)/(43), (42)/(44) and direct plus two-step J/ψ production processes in $\gamma^{12}\text{C}$ and $\gamma^{184}\text{W}$ interactions, calculated on the basis of Eqs. (24), (61) for laboratory polar angles of 0° – 20° and for incident photon lowest resonant energy of 9.44 GeV, are shown, respectively, in Figs. 9 and 10. The same as in these figures, but for initial highest photon resonant energy of 10.12, is presented in Figs. 11 and 12. The resonant momentum differential cross sections for the production of J/ψ mesons in the two-step processes $\gamma p \rightarrow P_{ci}^+ \rightarrow J/\psi p$ and $\gamma n \rightarrow P_{ci}^0 \rightarrow J/\psi n$ ($i = 1, 2, 3, 4$), proceeding on the intranuclear nucleons of carbon and tungsten target nuclei, were obtained for three employed values of the branching ratios $Br[P_{ci}^+ \rightarrow J/\psi p]$ and $Br[P_{ci}^0 \rightarrow J/\psi n]$. It can be seen from these figures that the total contribution to the J/ψ production on both these nuclei, coming from the intermediate P_{ci}^+ and P_{ci}^0 states decaying to the $J/\psi p$ and $J/\psi n$ modes with branching fractions of 0.25%, shows practically flat behavior, and it is significantly larger than that from the background processes (1), (2) in the "low"-momentum regions of 4.5–5.5 GeV/c and 4.5–6 GeV/c for considered photon beam energies of 9.44 and 10.12 GeV, respectively. As a result, in them the combined charmonium yield is completely governed by the presence of the P_{ci}^+ and P_{ci}^0 states in its production. Its strength is almost totally determined by the branching ratios $Br[P_{ci}^+ \rightarrow J/\psi p]$ and $Br[P_{ci}^0 \rightarrow J/\psi n]$ used in the calculations with a value, which is still large enough to be measured, as one may hope, at the CEBAF (cf. [13]), and which increases by a factor of about ten for both photon beam energies considered when going from carbon target nucleus to tungsten one ¹²⁾. This leads to the well separated and experimentally distinguishable differences between all combined calculations, corresponding to the adopted options for these ratios, for both target nuclei and for both photon energies considered. Since the J/ψ meson production differential cross sections at photon beam energy of 9.44 GeV are larger than those at the energy of 10.12 GeV by a factor of about 20 in the above "low"-momentum regions, their measurements on light and especially on heavy nuclear targets at photon energies in the "low"-energy resonance region will open an opportunity to determine accurately the above branching ratios – at least to distinguish between their realistic options of 0.25, 0.5 and 1%. Such measurements could also be performed in the future at the JLab in the framework of the proposed here E12-12-006 experiment [5, 17].

¹²⁾It is interesting to note that the photoproduction of J/ψ - ^3He bound state ($[^3\text{He}]_{J/\psi}$) on a ^4He target has been investigated in Ref. [29] using the impulse approximation, several $\gamma + N \rightarrow J/\psi + N$ models based on the Pomeron-exchange and accounting for the pion-exchange mechanism at low energies, and various J/ψ -nucleus potentials. The upper boundary of the predicted total cross sections was found to be very small – it is about 0.1–0.3 pb. The possibility of photoproduction of a six quark- J/ψ bound state ($[q^6]_{J/\psi}$) on the ^3He target has been studied in Ref. [29] as well. The upper boundary of the predicted total cross sections of $\gamma + ^3\text{He} \rightarrow [q^6]_{J/\psi} + N$ was obtained to be slightly larger than in the preceding case – it is about 2–4 pb, depending on the model of $\gamma + N \rightarrow J/\psi + N$ used in the calculations. These predictions may facilitate the planning of possible measurements of $[^3\text{He}]_{J/\psi}$ and $[q^6]_{J/\psi}$ bound states at JLab.

Accounting for the above considerations, we can conclude that the near-threshold J/ψ energy and momentum distribution measurements in photon-induced reactions both on protons and on nuclear targets will provide further evidence for the existence of the pentaquark P_{ci}^+ , P_{ci}^0 resonances, and will shed light on their decay rates to the channels $J/\psi p$ and $J/\psi n$.

4. Epilogue

In this paper we studied the near-threshold J/ψ meson photoproduction from protons and nuclei by considering incoherent direct non-resonant ($\gamma p \rightarrow J/\psi p$, $\gamma n \rightarrow J/\psi n$) and two-step resonant ($\gamma p \rightarrow P_{ci}^+ \rightarrow J/\psi p$, $\gamma n \rightarrow P_{ci}^0 \rightarrow J/\psi n$, $i = 1, 2, 3, 4$; $P_{c1}^{+,0} = P_c^{+,0}(4312)$, $P_{c2}^{+,0} = P_c^{+,0}(4337)$, $P_{c3}^{+,0} = P_c^{+,0}(4440)$, $P_{c4}^{+,0} = P_c^{+,0}(4457)$) charmonium production processes. We have calculated the absolute excitation functions, energy and momentum distributions for the non-resonant, resonant and for the combined (non-resonant plus resonant) production of J/ψ mesons on protons as well as, using the nuclear spectral function approach, on carbon and tungsten target nuclei at near-threshold incident photon energies by assuming the spin-parity assignments of the hidden-charm resonances $P_c^{+,0}(4312)$, $P_c^{+,0}(4337)$, $P_c^{+,0}(4440)$ and $P_c^{+,0}(4457)$ as $J^P = (1/2)^-$, $J^P = (1/2)^-$, $J^P = (1/2)^-$ and $J^P = (3/2)^-$ within three different realistic scenarios for the branching ratios of their decays to the $J/\psi p$ and $J/\psi n$ modes (0.25, 0.5 and 1%). It was shown that will be very hard to measure the P_{ci}^+ pentaquark states through the scan of the J/ψ total photoproduction cross section on a proton target in the near-threshold energy region around the resonant photon energies of 9.44, 9.554, 10.04 and 10.12 GeV if these branching ratios $\sim 1\%$ and less. It was also demonstrated that at these photon beam energies the J/ψ energy and momentum combined distributions considered reveal distinct sensitivity to the above scenarios, respectively, at "low" J/ψ total energies and momenta, which implies that they may be an important tool to provide further evidence for the existence of the pentaquark P_{ci}^+ and P_{ci}^0 resonances and to get valuable information on their decay rates to the $J/\psi p$ and $J/\psi n$ final states. The measurements of these distributions could be performed in the near future at the JLab in Hall A within the planned here high-statistics ($\sim 800k$ J/ψ events in photoproduction) and high-precision E12-12-006 experiment using the SoLID detector.

References

- [1] R. Aaij *et al.* (LHCb Collaboration), Phys. Rev. Lett. **115**, 072001 (2015); arXiv:1507.03414 [hep-ex].
- [2] R. Aaij *et al.* (LHCb Collaboration), Phys. Rev. Lett. **122**, 222001 (2019); arXiv:1904.03947 [hep-ex].
- [3] R. Aaij *et al.* (LHCb Collaboration), Phys. Rev. Lett. **128**, 062001 (2022); arXiv:2108.04720 [hep-ex].
- [4] A. Ali *et al.* (The GlueX Collaboration), Phys. Rev. Lett. **123**, 072001 (2019); arXiv:1905.10811 [nucl-ex].
- [5] J. Arrington *et al.*, arXiv:2112.00060 [nucl-ex].
- [6] E. Ya. Paryev and Yu.T. Kiselev, Nucl. Phys. A **978**, 201 (2018); arXiv:1810.01715 [nucl-th].
- [7] E. Ya. Paryev, Nucl. Phys. A **996**, 121711 (2020); arXiv:2003.00788 [nucl-th].

- [8] E. Ya. Paryev and Yu.T. Kiselev, Phys. At. Nucl. **81** (5), 566 (2018).
- [9] E. Ya. Paryev, Yu. T. Kiselev and Yu. M. Zaitsev, Nucl. Phys. A **968**, 1 (2017).
- [10] E. Ya. Paryev, Nucl. Phys. A **1023**, 122452 (2022);
arXiv:2205.00728 [hep-ph].
- [11] S. V. Efremov and E. Ya. Paryev, Eur. Phys. J. A **1**, 99 (1998).
- [12] E. Ya. Paryev, Eur. Phys. J. A **7**, 127 (2000).
- [13] B. Duran *et al.*, arXiv:2207.05212 [nucl-ex].
- [14] S. J. Brodsky, E. Chudakov, P. Hoyer and J. M. Laget, Phys. Lett. B **498**, 23 (2001).
- [15] T. Gutsche and V. E. Lyubovitskij, Phys. Rev. D **100**, 094031 (2019);
arXiv:1910.03984 [hep-ph].
- [16] X.-Y. Wang, J. He, X.-R. Chen, Q. Wang, and X. Zhu, Phys. Lett. B **797**, 134862 (2019);
arXiv:1906.04044 [hep-ph].
- [17] S. Joosten. Quarkonium production near threshold at JLab and EIC,
9th Workshop of the APS Topical Group on hadron physics (2021).
URL <https://indico.jlab.org/event/412/contributions/8266/attachments/6888/9385/20210416-GHP-Jpsi-Threshold.pdf>
- [18] X. Cao, J.-P. Dai, Phys. Rev. D **100**, 054033 (2019);
arXiv:1904.06015 [hep-ph].
- [19] M. Karliner and J. L. Rosner, Phys. Lett. B **752**, 329 (2016);
arXiv:1508.01496 [hep-ph].
- [20] X.-Y. Wang, X.-R. Chen, and J. He, Phys. Rev. D **99**, 114007 (2019).
- [21] C.-J. Xiao *et al.*, Phys. Rev. D **100**, 014022 (2019).
- [22] H. X. Chen, W. Chen and S.-L. Zhu, Phys. Rev. D **100**, 051501 (2019);
arXiv:1903.11001 [hep-ph].
- [23] A. N. Hiller Blin *et al.*, Phys. Rev. D **94**, 034002 (2016);
arXiv:1606.08912 [hep-ph].
- [24] E. Ya. Paryev, Chinese Physics C, Vol. **44**, No. (10), 104101 (2020);
arXiv:2007.01172 [nucl-th].
- [25] Q. Wang, X.-H. Liu, and Q. Zhao, Phys. Rev. D **92**, 034022 (2015);
arXiv:1508.00339 [hep-ph].
- [26] J. J. Wu, T.-S. H. Lee, and B. S. Zou, Phys. Rev. C **100**, 035206 (2019);
arXiv:1906.05375 [nucl-th].
- [27] Y. Huang, J. He, H.-F. Zhang, and X.-R. Chen, J. Phys. G: Nucl. Part. Phys. **41**, 115004 (2014);
arXiv:1305.4434 [nucl-th].

- [28] M.-L. Du, V. Baru, F.-K. Guo, C. Hanhart, U.-G. Meissner, A. Nefediev, I. Strakovsky, Eur. Phys. J. C **80**, 1053 (2020);
arXiv:2009.08345 [hep-ph].
- [29] J. J. Wu and T.-S. H. Lee, Phys. Rev. C **86**, 065203 (2012);
arXiv:1210.6009 [nucl-th].